

**QIRT
2012**

1

39

Title

**IR THERMOGRAPHY IN FLUID MECHANICS AND
HEAT TRANSFER**

BY

G. HETSRONI

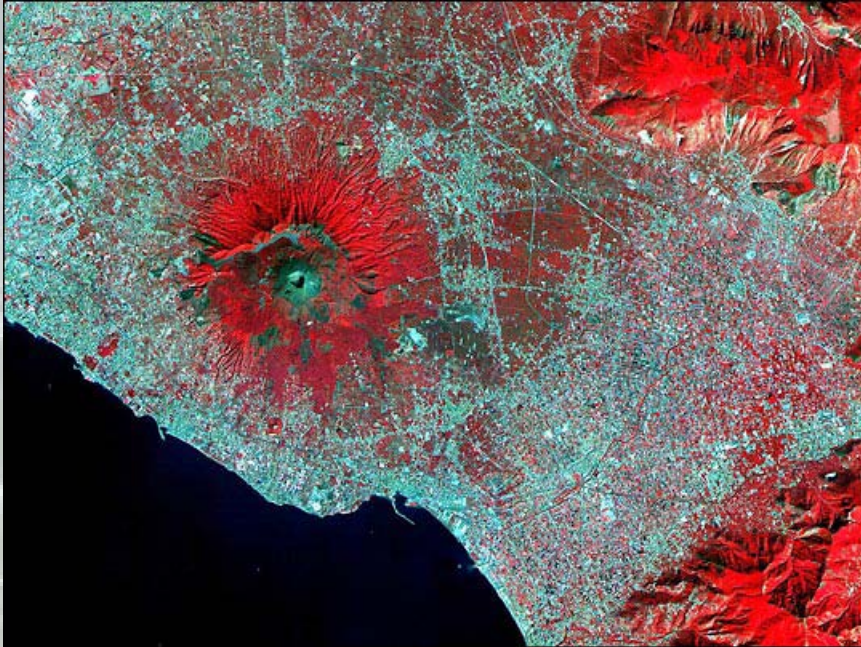
**DANCIGER PROFESSOR OF ENGINEERING
TECHNION – ISRAEL INSTITUTE OF TECHNOLOGY**

**QIRT
2012**

2

39

Introduction



This Advanced Spaceborne Thermal Emission and Reflection Radiometer (ASTER) image of Mt. Vesuvius, Italy was acquired September 26, 2000. The full-size false-color image covers an area of 36 by 45 km. Vesuvius overlooks the city of Naples and the Bay of Naples in central Italy. (Popocatepetl and Mount Fuji are other volcanos surrounded by dense urban areas.) In 79 AD, Vesuvius erupted cataclysmically, burying all of the surrounding cities with up to 30 m of ash. The towns of Pompeii and Herculanaeum were rediscovered in the 18th century, and excavated in the 20th century. They provide a snapshot of Roman life from 2000 years ago: perfectly preserved are wooden objects, food items, and the casts of hundreds of victims. Vesuvius is intensively monitored for potential signs of unrest that could signal the beginning of another eruption

**QIRT
2012**

3

39



This lecture is in honor of
Giovanni Maria Carlomagno
for his many contributions to fluid
Mechanics and Thermography

**QIRT
2012**

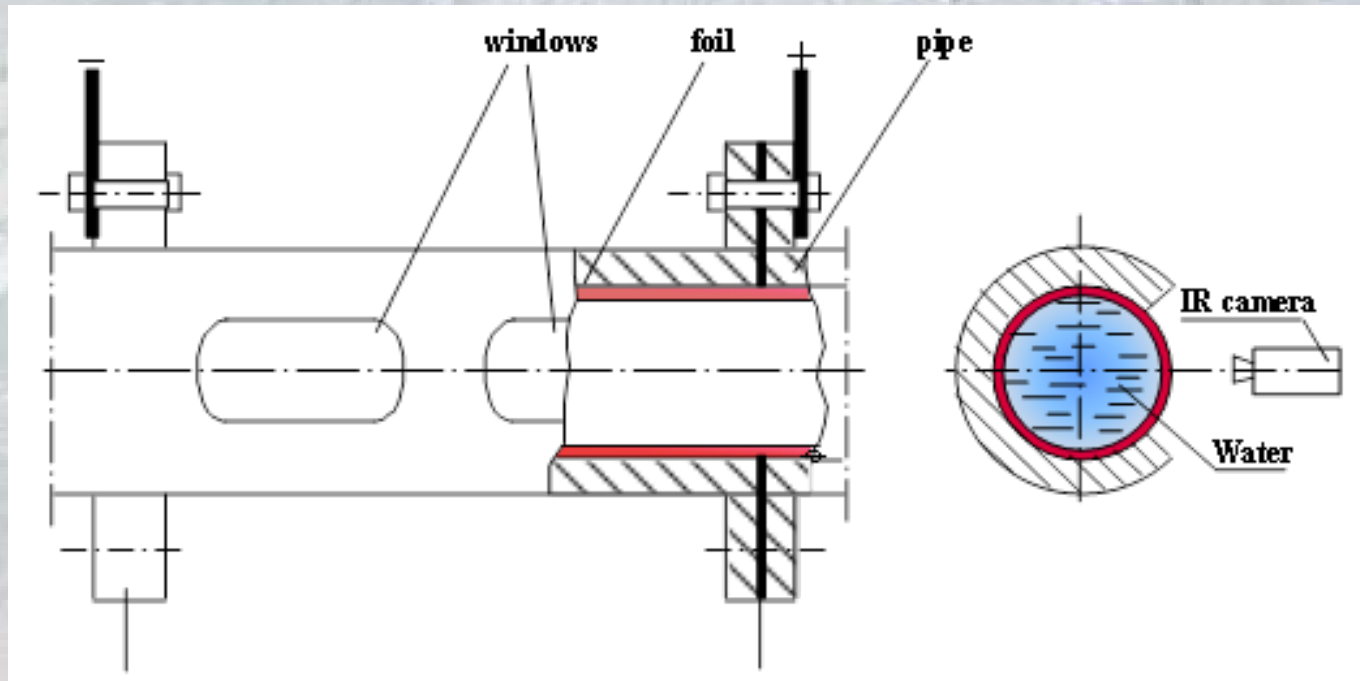
4

39

Content

- 1. Methodology of thin film IR measurements.**
- 2. Detection of coherent structures in single-phase flow.**
- 3. Liquid-air flow. Thermal pattern on the heated wall.**
- 4. Pool boiling. Temperature field on a horizontal surface.**
- 5. Flow boiling in a capillary tube. Thermal entrance region. Dryout.**
- 6. Micro-channels. IR measurements of the heated wall and the fluid temperatures.**
- 7. Conclusions.**

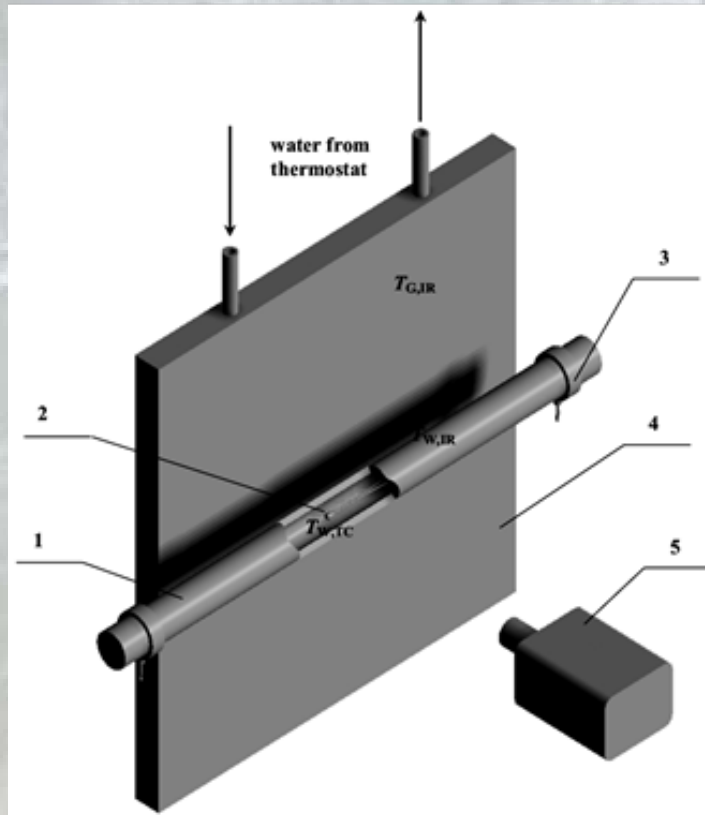
METHODOLOGY OF THIN FILM INFRARED MEASUREMENT



The IR camera is placed in the vicinity of the heated foil. A very thin foil makes it possible to increase frequency response of the IR measurements.

G. Hetsroni, R. Rozenblit & L.P. Yarin 1996 A hot-foil infrared technique for studying the temperature field of a wall. *Meas. Sci. Technol.* 7: 1418-1427

Temperature measurements on the surface of capillary tubes



The method is based on compensating the background radiation by controlling its temperature to the same level of the temperature of the capillary tube. This is achieved by recording the infrared data against a background, whose temperature was maintained at a given value by a thermostat.

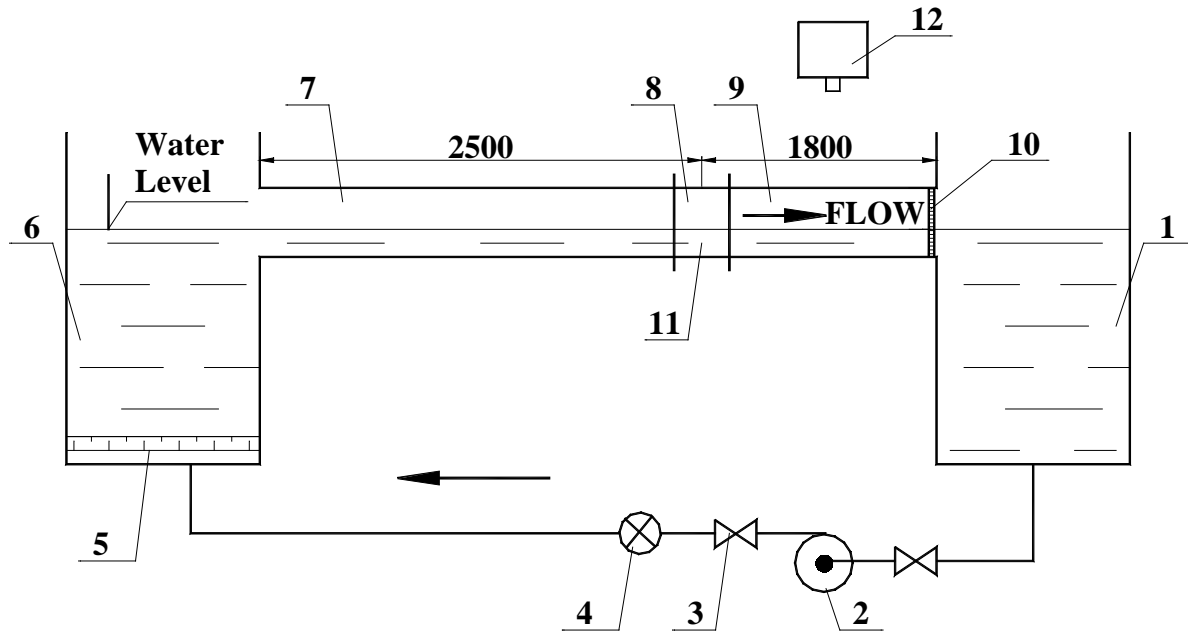
Scheme of infrared measurement of surface temperature capillary tube and calibration method.

1. Calibration section,
2. Thermocouple,
3. Electrical contacts,
4. Screen (background),
5. IR video camera.

G. Hetsroni, M. Gurevich, A. Mosyak, R. Rozenblit, 2003 Surface temperature measurement of a heated capillary tube by means of an infrared technique. *Measurement Science and Technology* 14, 807- 814

METHODOLOGY OF INFRARED MEASUREMENT

Measurements on the water surface



1 exit tank, 2 pump, 3 flow control valve, 4 flowmeter, 5 grid, 6 entrance tank, 7 development section, 8 test section, 9 section of thermal spots visual detection, 10 wave absorber, 11 heated wire, 12 IR camera

G. Hetsroni, A. Mosyak, 1996 Bursting process in turbulent boundary layers at low Reynolds numbers. *Chem. Eng. Comm.* 148-150, 85-104

The purpose of this study was to connect the coherent structures, at the location of their formation at the boundary layer, to their appearance on the surface.

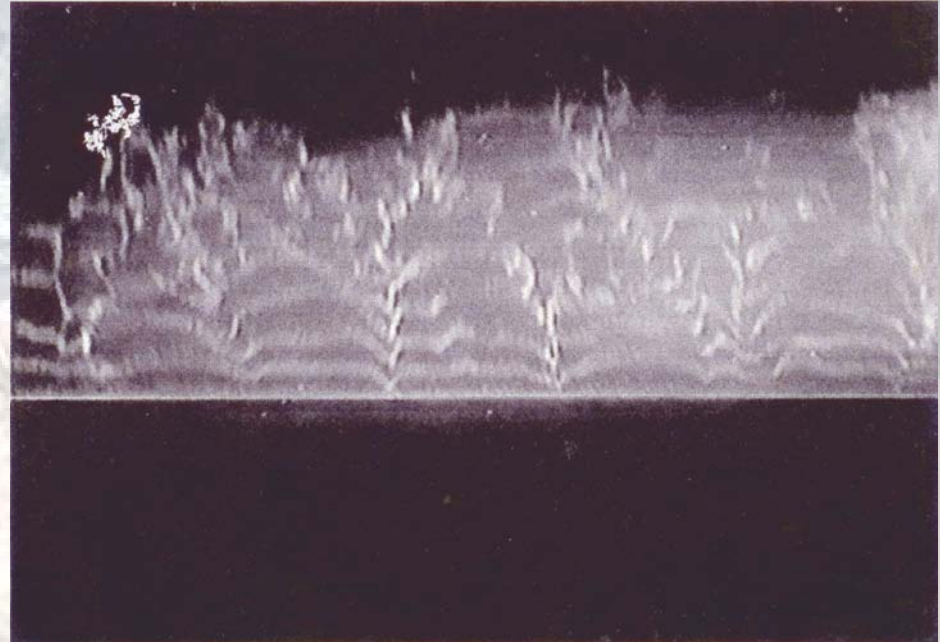
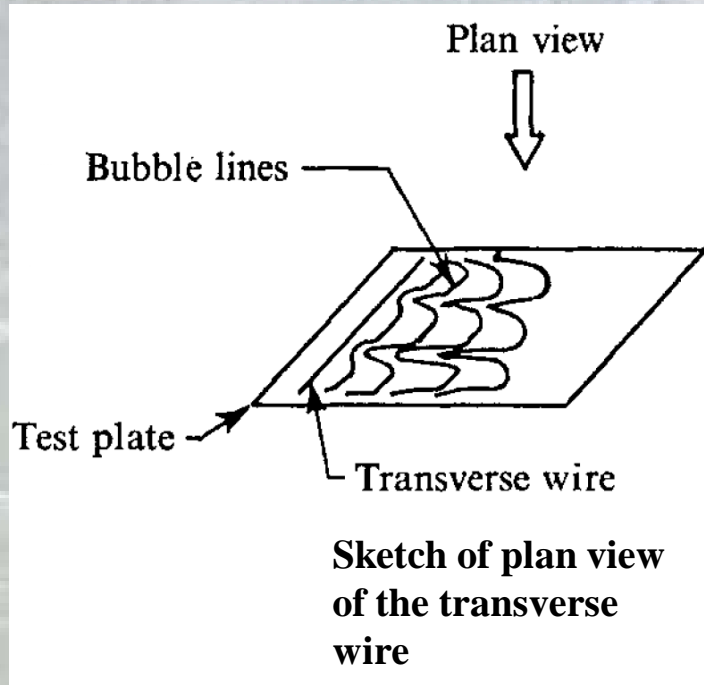
There is also an additional physical insight which can be gleaned from the spots emergence on the water surface: the surface-renewal motions originate in the bursting motions which occur in the buffer region. That is, fluid which is strongly listed towards the outer layer almost always arrives by the bursting at the free surface and renews the free surface.

**QIRT
2012**

8

39

BURSTING PROCESS IN TURBULENT BOUNDARY LAYER



In the flow-visualization studies by Kline et al. (1967) it was shown that in the near-wall region of bounded turbulent flows, there are low-velocity streaks, and subsequent ejections of the low-velocity fluid to the outer region of the flow. There are several stages in the process by which low-velocity streaks are eventually ejected away from the wall. The total process was called a “burst”.

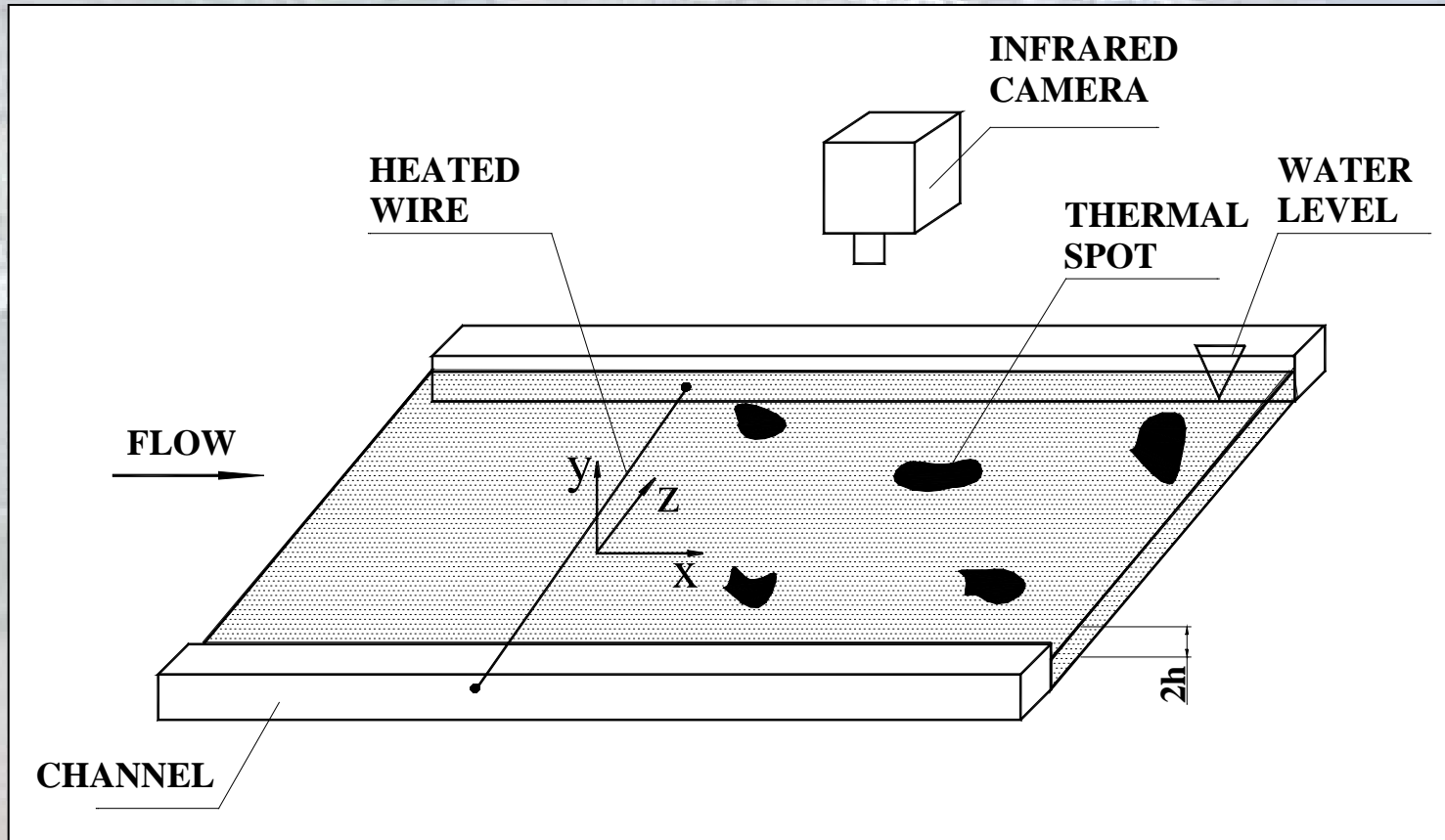
Kline, S.J., Reynolds, W.C., Schraub, F.A., & Runstadler, P.W. 1967, The structure of turbulent boundary layers. *J. Fluid Mech.*, 30,741-773

QIRT
2012

9
39

BURST DETECTING BY IR

Schematic diagram of the visual bursting detection



There is physical insight which can be gleaned from the spots emergence on the water surface. The surface-renewal motions originate in the bursting motions which occur in the buffer region.

G. Hetsroni, A. Mosyak 1996 Bursting process in turbulent boundary layer at low Reynolds numbers. *Chem.Eng. Comm.* 148-150, 85-104

**QIRT
2012**

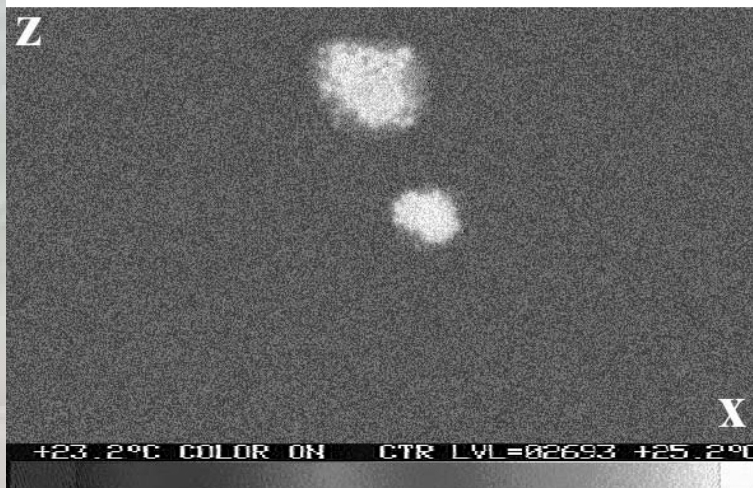
10
39

BURST DETECTING BY IR

Image analysis



a



b

**Thermal spots on the water surface:
a single burst event,
b thermal spots from two ejections**

From the video recording we counted the number of new spots N_x as they appeared on the interface in the band $z^+=\pm 50$ at the center of the flume. The spot frequency was $f_s=N_x/t_{sm}$, where t_{sm} is the sampling interval. As the time between bursts in the present study was from 2 to 6 s a sampling frequency of 25 Hz was chosen, with a sampling time of 1,500 s. We also counted the number of spots, $N_{x,z}$, which appeared over the whole width of the interface. The spot frequency per unit of span was calculated as $F_s=N_{x,z}/(z\times t_{sm})$.

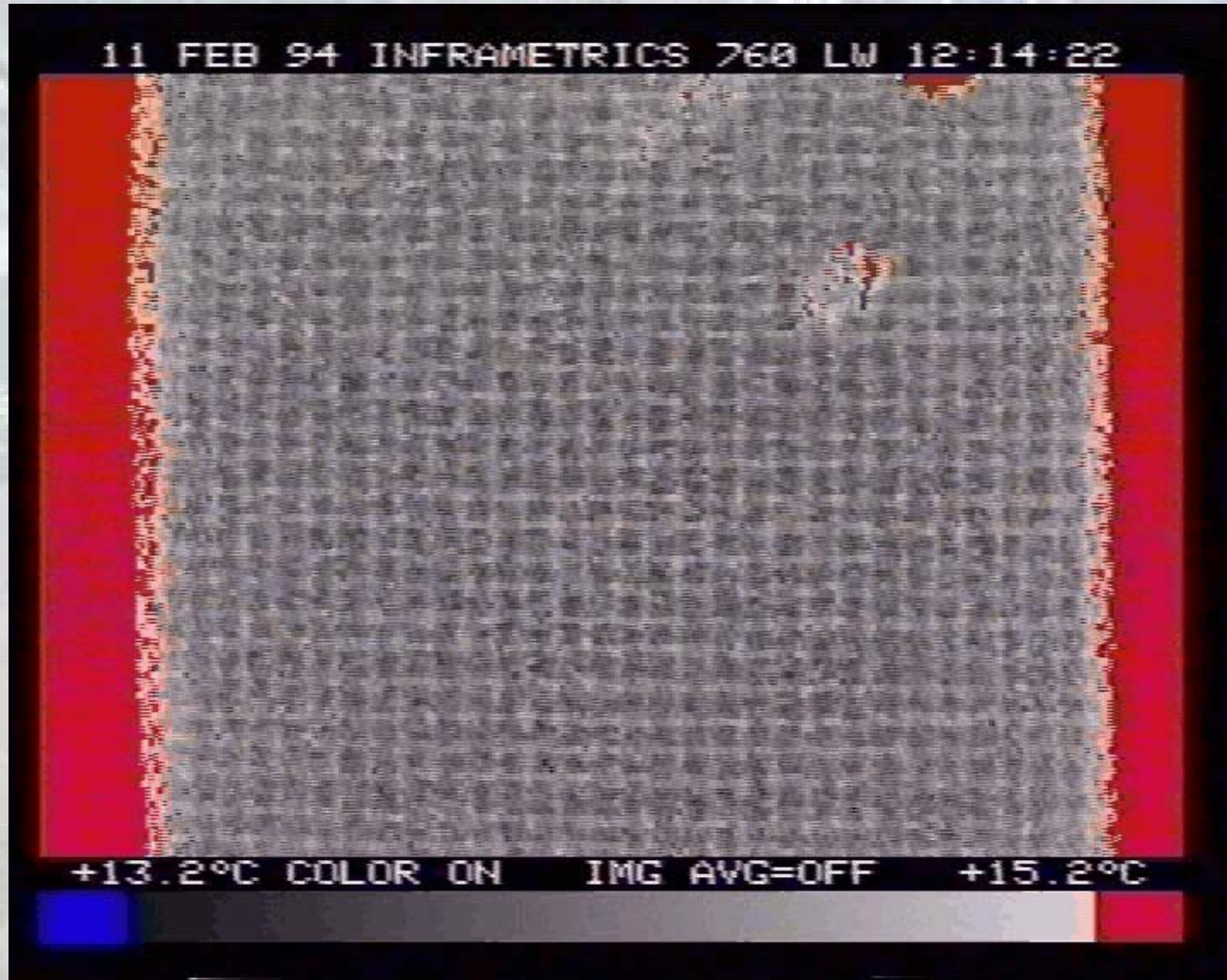
**QIRT
2012**

11

39

BURST DETECTING BY IR

Visualization



**QIRT
2012**

12
39

BURST DETECTING BY IR

Experimental results

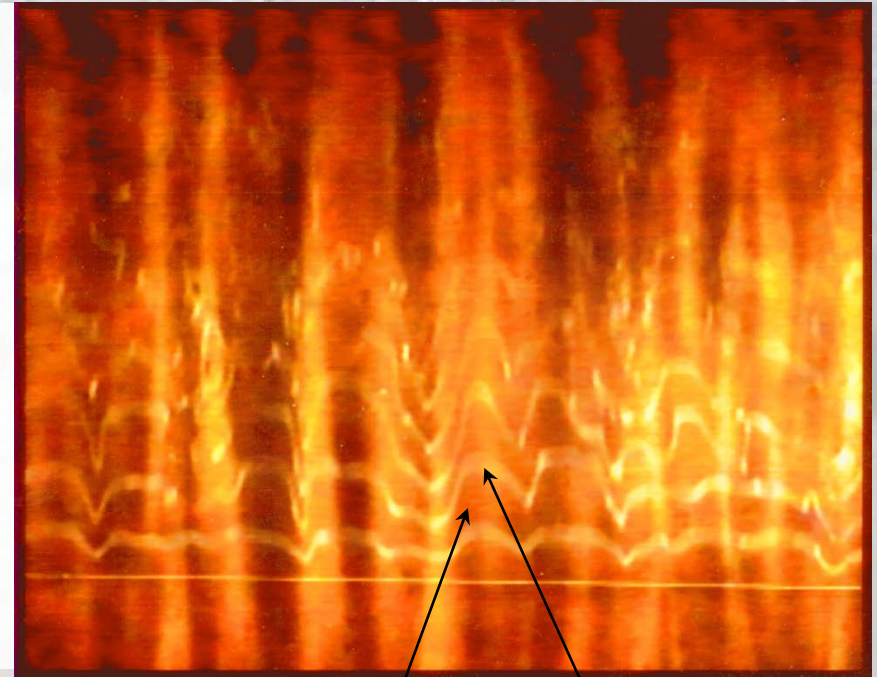
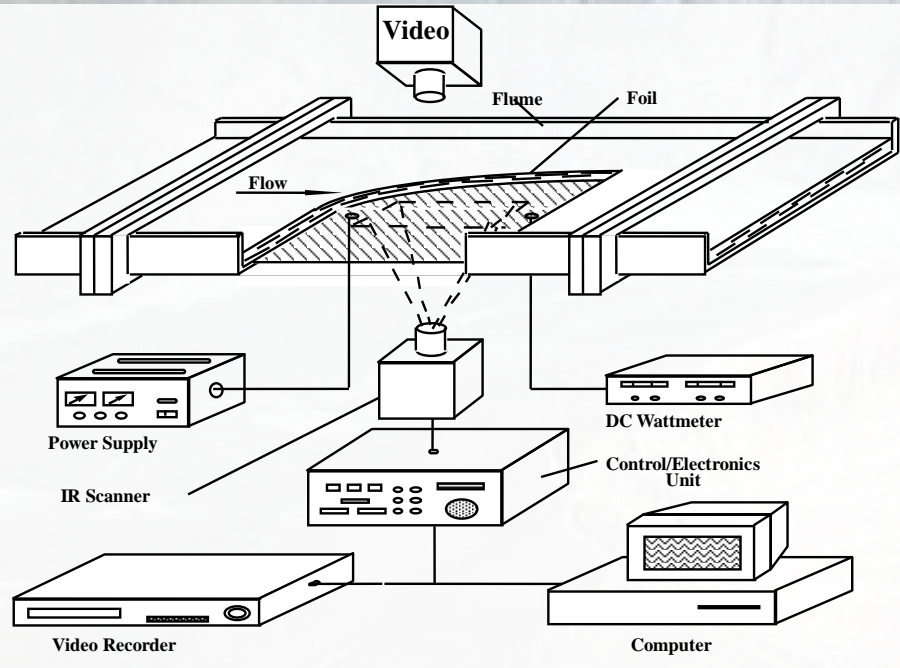
| Fluid | Flow depth, 2h (m) | Reynolds number Re $Re = \frac{U2h}{\nu}$ | Wall shear velocity u^* $u^* = \sqrt{\tau_w / \rho}$ (m/s) | Percent of drag reduction $Dr, (\%)$ | Bursting frequency $f^+ = \frac{\nu}{tu^{*2}}$ | Bursting rate per meter, F (bursts/ms) |
|------------------------------------|--------------------|--|--|---|---|---|
| Water | 0.037 | 4,200 | 0.0070 | | 0.0102 | 30 |
| | | 4,800 | 0.0077 | | 0.0107 | 46 |
| | | 7,100 | 0.011 | | 0.0103 | 130 |
| | | 12,000 | 0.017 | | 0.0110 | 550 |
| | 0.050 | 3,100 | 0.0042 | | 0.0104 | 6.7 |
| | 0.085 | 4,700 | 0.0035 | | 0.0108 | 4.0 |
| | 0.093 | 9,900 | 0.0060 | | 0.0100 | 19 |
| 530 ppm by weight Habon G solution | 0.037 | 3,700 | 0.0051 | 46 | 0 | 0 |
| | | 4,200 | 0.0054 | 50 | | |
| | | 6,200 | 0.0078 | 50 | | |
| | | 10,000 | 0.012 | 53 | | |

$$Dr = \frac{\Delta P_{water} - \Delta P_{surf}}{\Delta P_{water}} \cdot 100$$

**QIRT
2012**

13
39

CONNECTION BETWEEN LOW VELOCITY LIQUID STREAKS AND TEMPERATURE STREAKS



Low temperature streak

High speed streak

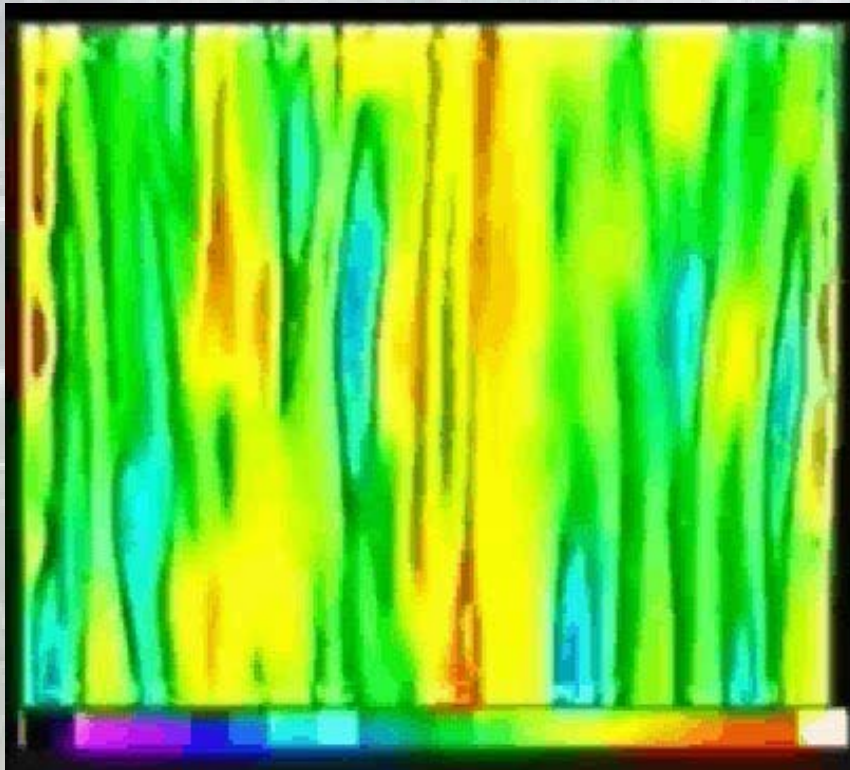
G. Hetsroni and R. Rozenblit 1994 Heat transfer to liquid-solid mixture in a flume.
Int. J. Multiphase Flow 20(4): 671-689

**QIRT
2012**

14
39

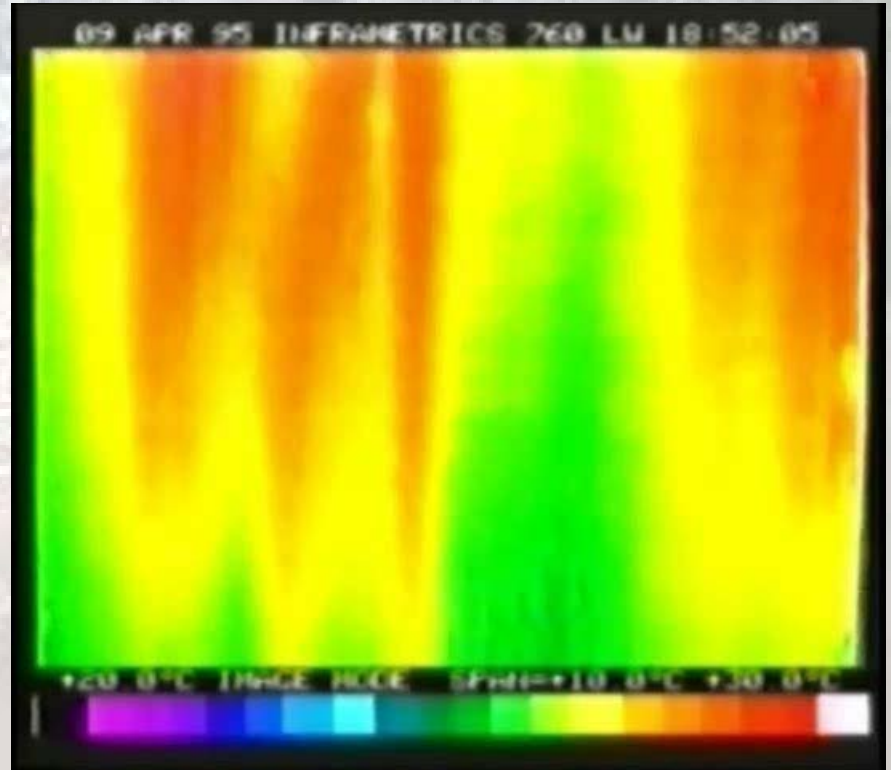
EFFECT OF SURFACTANTS ON THERMAL STREAKS

Drag reduction solution



Water

Re = 5500



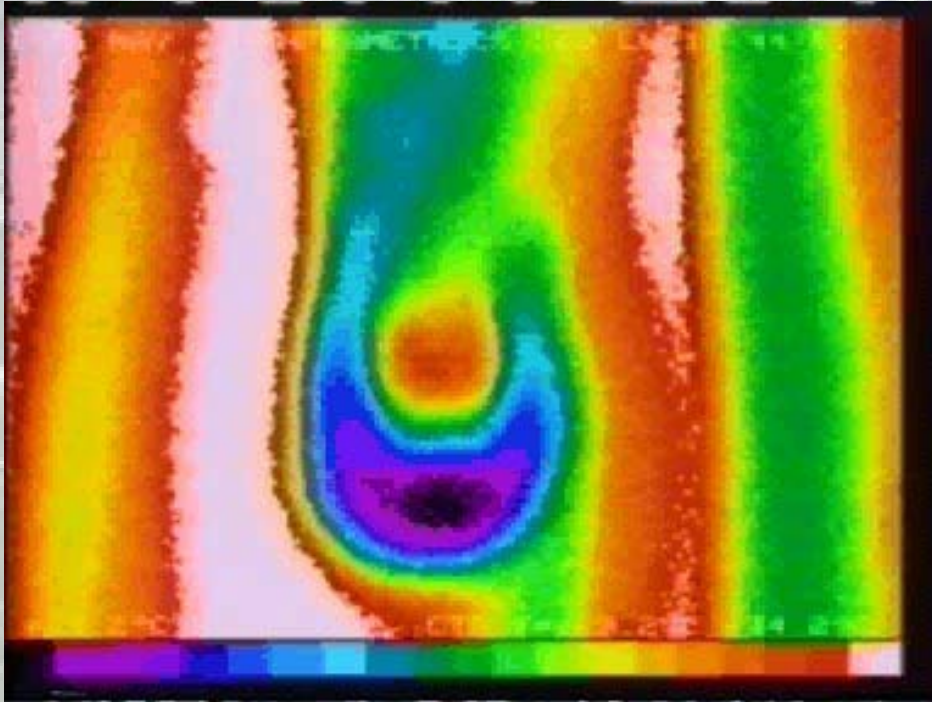
Habon G, C=0.027%

**QIRT
2012**

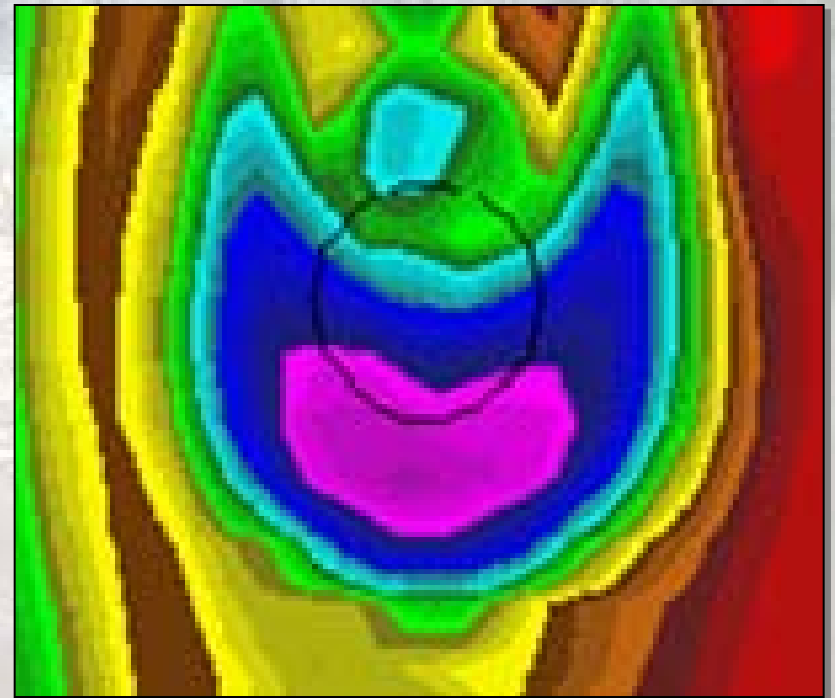
15
39

THERMAL PATTERN. SINGLE COARSE PARTICLE

$d^+=34$, $C_v=4 \cdot 10^{-4}$, $Re=2600$



experiment



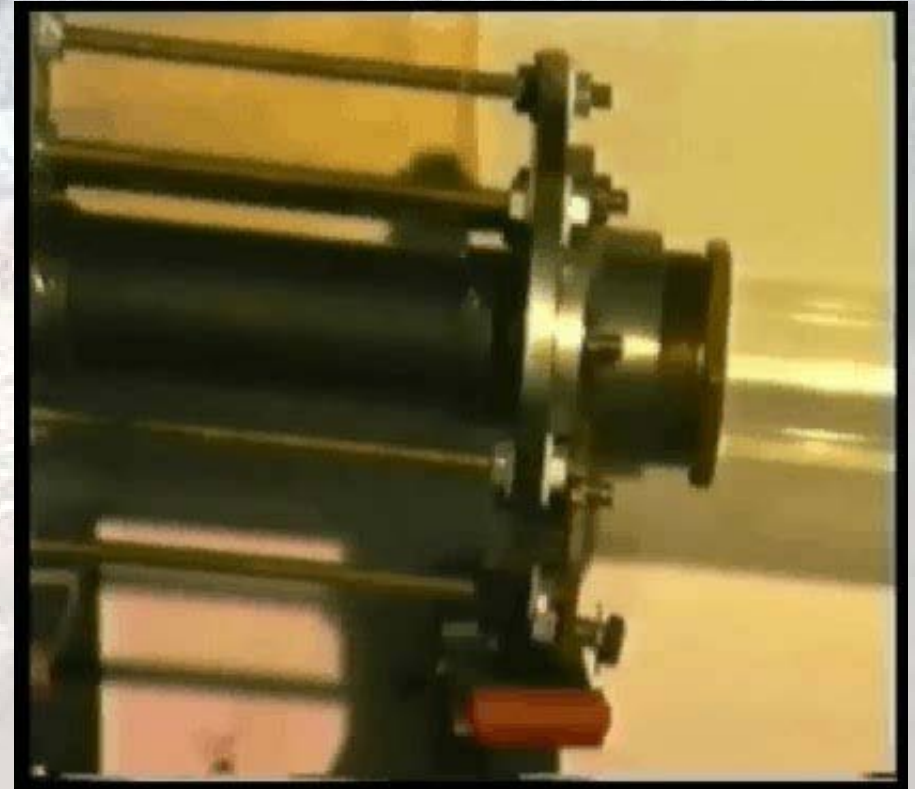
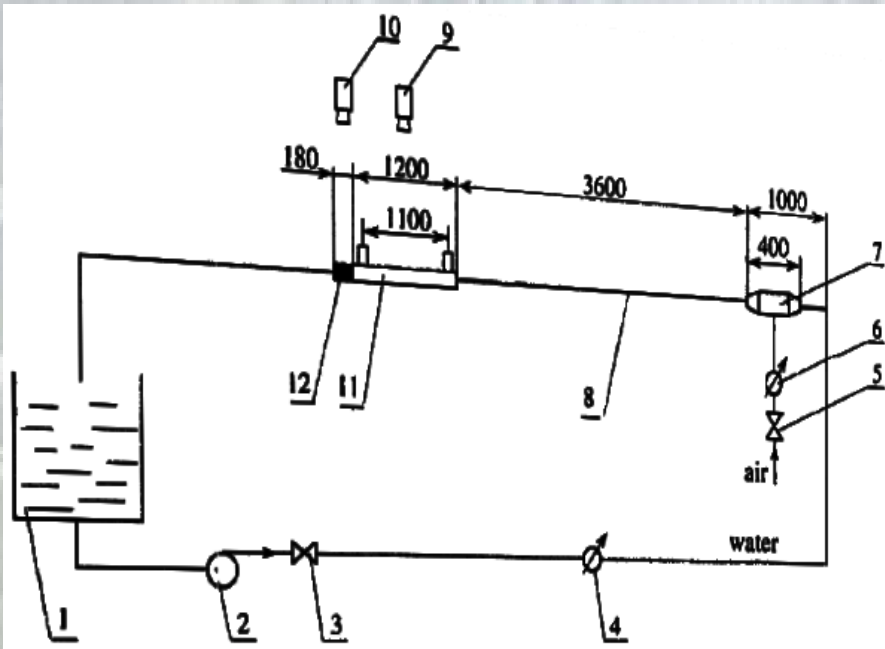
DNS

**QIRT
2012**

16
39

THERMAL PATTERN ON THE HEATED WALL IN AIR-WATER FLOW

Inclined tube Experimental setup



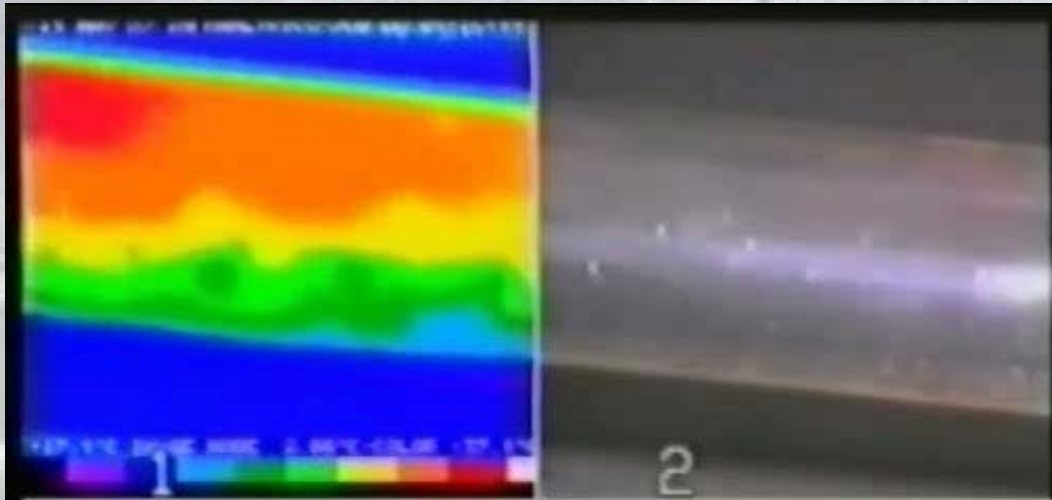
1. tank; 2. pump; 3. flow regulator; 4. water flowmeter; 5. air regulator; 6. air flowmeter; 7. mixing section; 8. development section; 9. video camera; 10. IR camera; 11. pressure measurement section; 12. heated test section

**QIRT
2012**

17
39

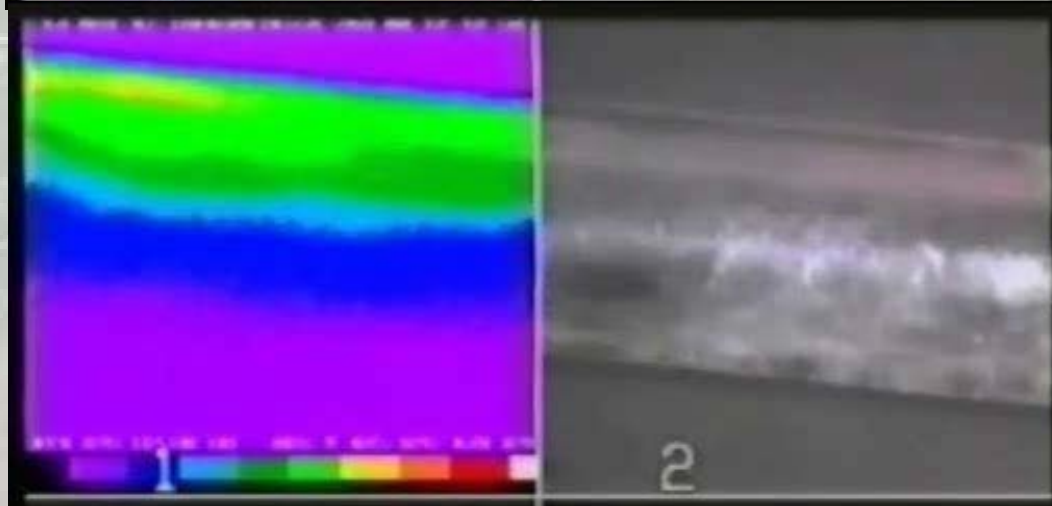
THERMAL PATTERN ON THE HEATED WALL IN AIR-WATER FLOW

Thermal and flow visualization



Unclosed flow

Open annular flow with disturbance waves. Dryout on the upper part of the pipe may be associated with open annular flow with motionless or slowly moving droplets



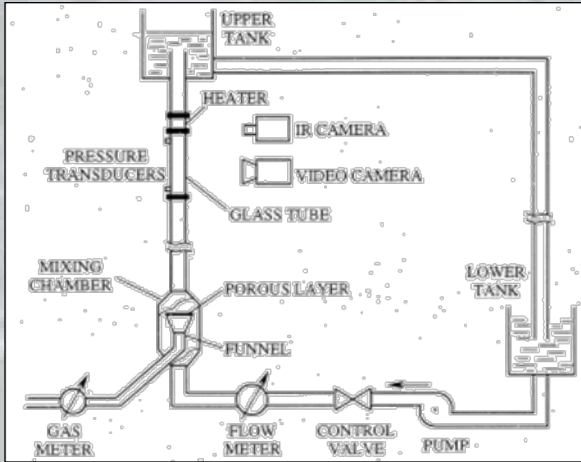
Closed flow

Closed annular flow with air-water clusters and liquid film on the upper part of the tube. Time and space average heat transfer coefficient is about 3-8 times higher than that for unclosed flow

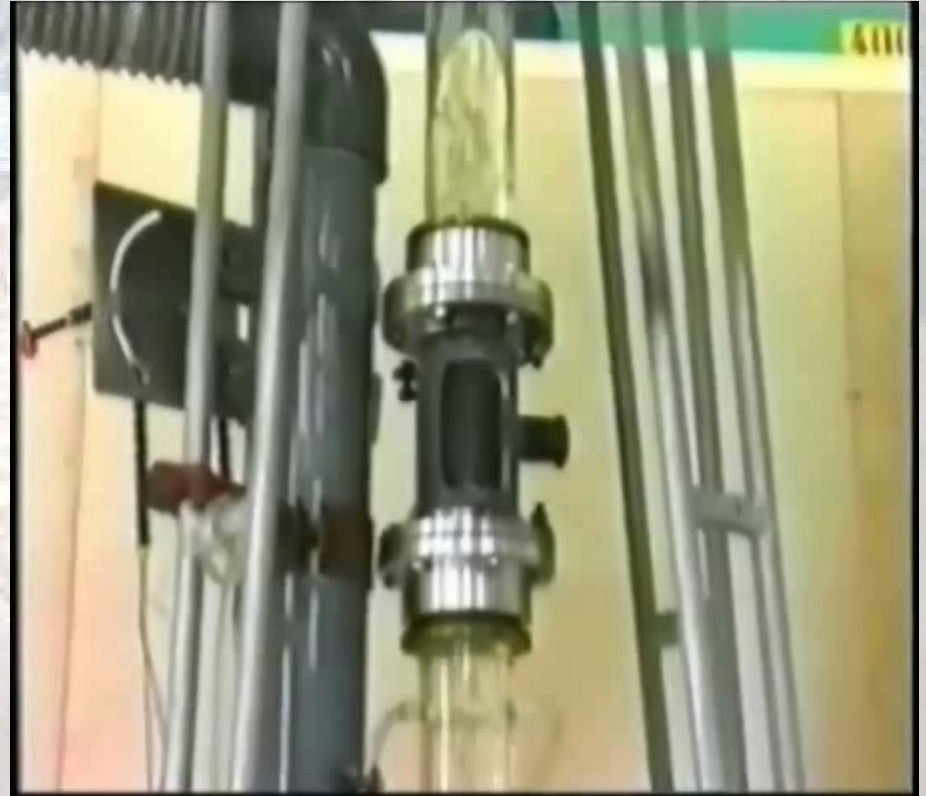
**QIRT
2012**

18
39

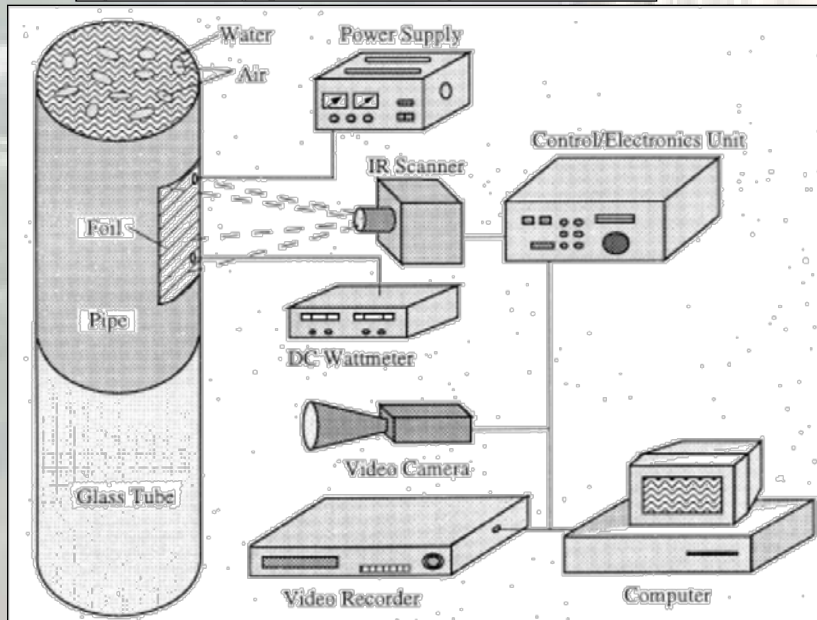
THERMAL PATTERN ON THE HEATED WALL IN AIR-WATER FLOW



Vertical tube Experimental setup



The upper part of the vertical tube



**QIRT
2012**

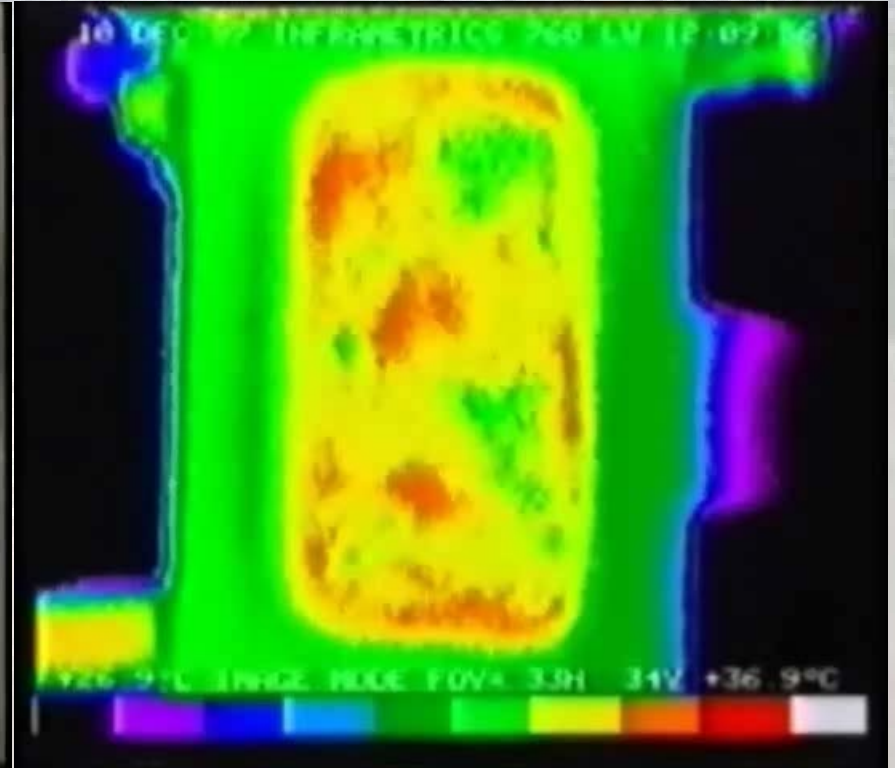
19
39

THERMAL PATTERN ON THE HEATED WALL IN AIR-WATER FLOW

Flow and thermal visualization



Bubble flow



IR image

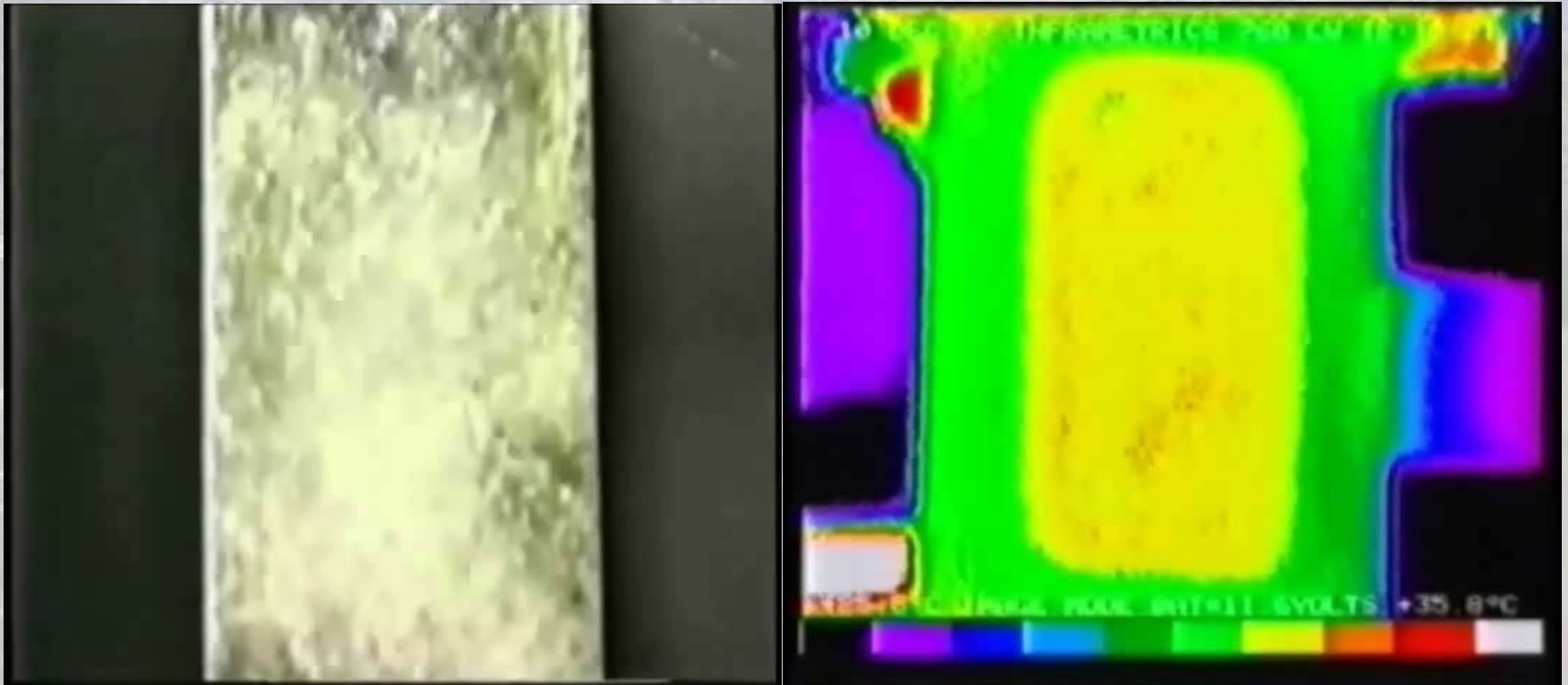
For the bubble flow, the streaky structure is destroyed. This phenomenon is accompanied by significant increase in the heat transfer coefficient

**QIRT
2012**

20
39

THERMAL PATTERN ON THE HEATED WALL IN AIR-WATER FLOW

Flow and thermal visualization



Slug flow

IR image

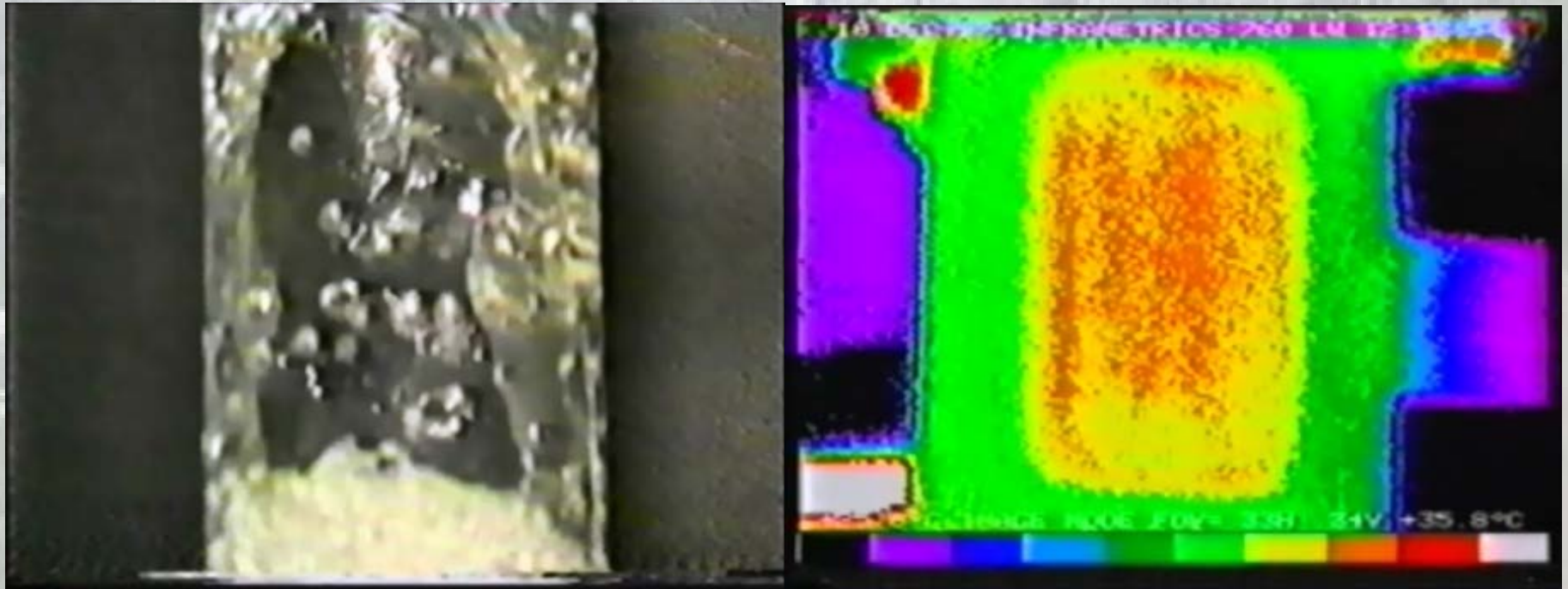
The temperature distribution on the heated wall depends strongly on whether water containing small gas bubbles (slug) or water surrounding the Taylor bubbles passes the heated wall at any instant

**QIRT
2012**

21
39

THERMAL PATTERN ON THE HEATED WALL IN AIR-WATER FLOW

Flow and thermal visualization. Still pictures



Taylor bubble

IR image

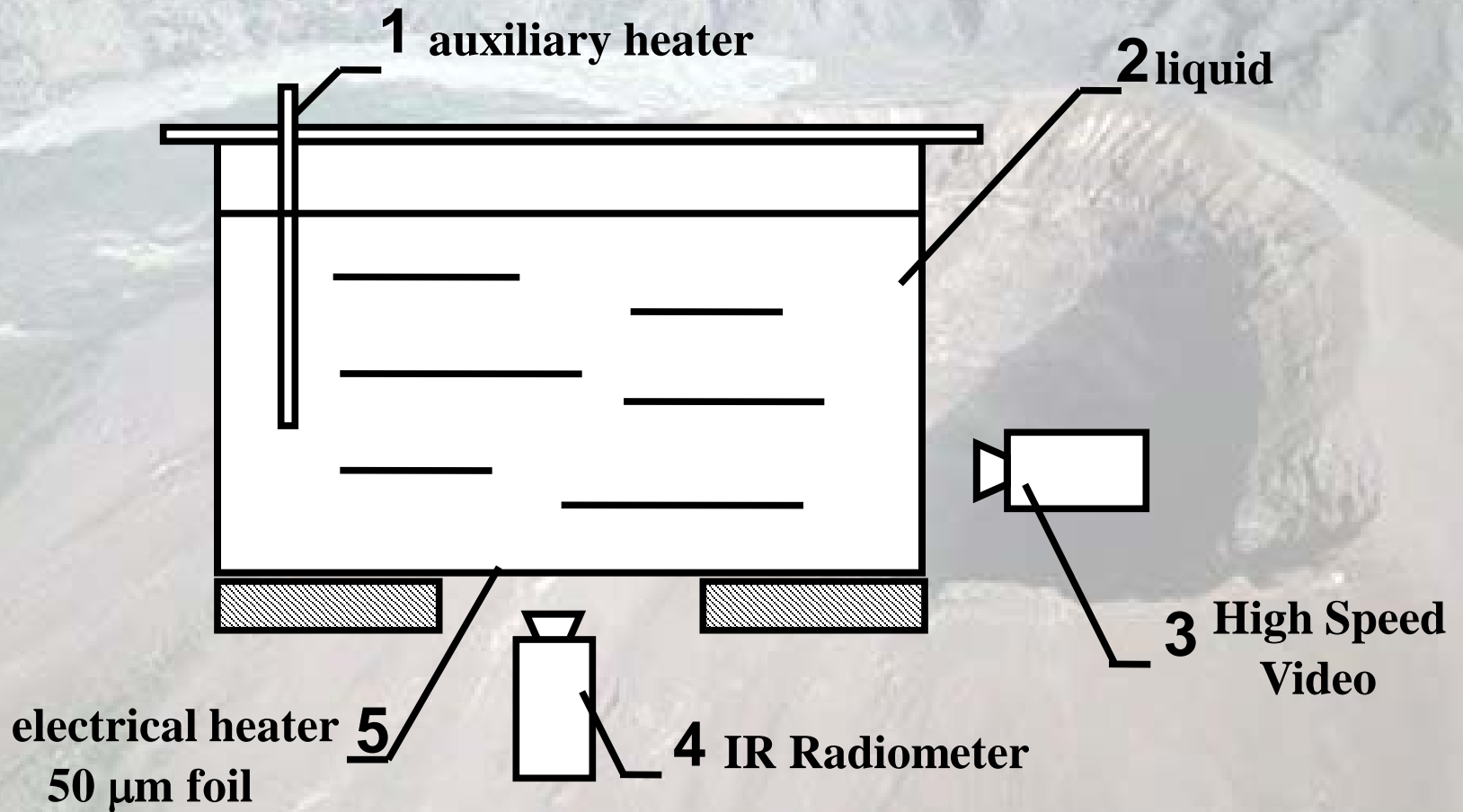
In the vicinity of Taylor bubble temperature of the heated wall increases

**QIRT
2012**

22
39

POOL BOILING

SATURATED BOILING ON THE HORIZONTAL HEATER MADE OF THIN FOIL. EXPERIMENTAL FACILITY

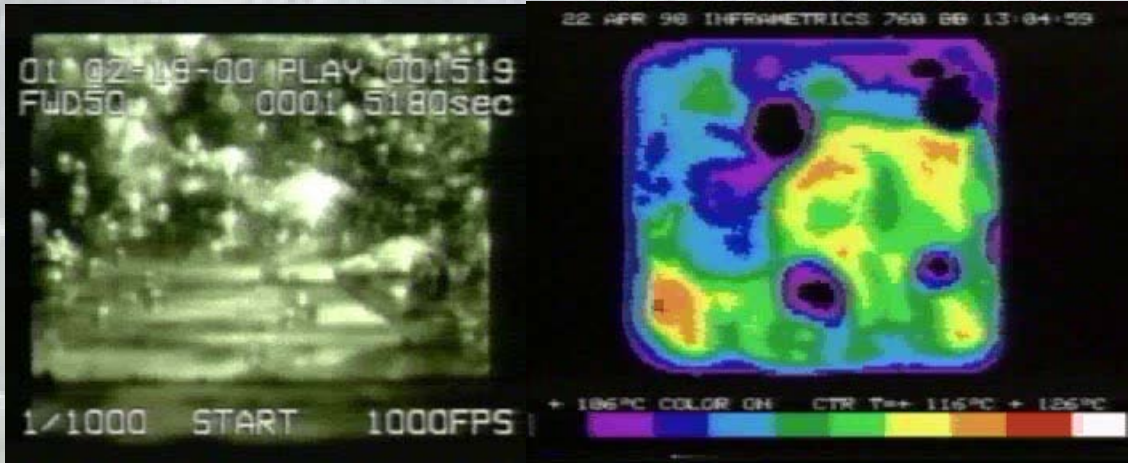


**QIRT
2012**

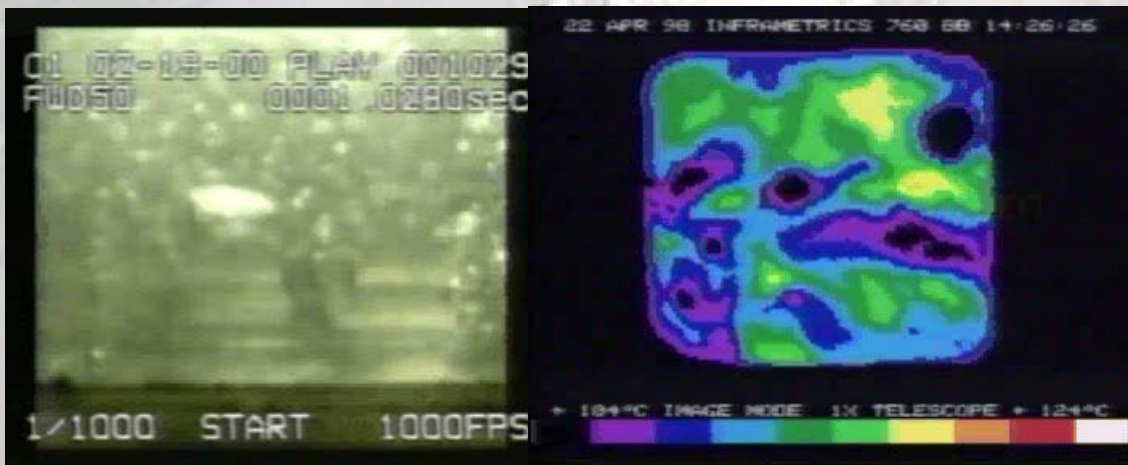
23
39

POOL BOILING

BUBBLE DYNAMICS AND TEMPERATURE FIELD ON THE HEATER



Water, $q=100 \text{ kW/m}^2$



**Habon G, 530 ppm
 $q=100 \text{ kW/m}^2$**

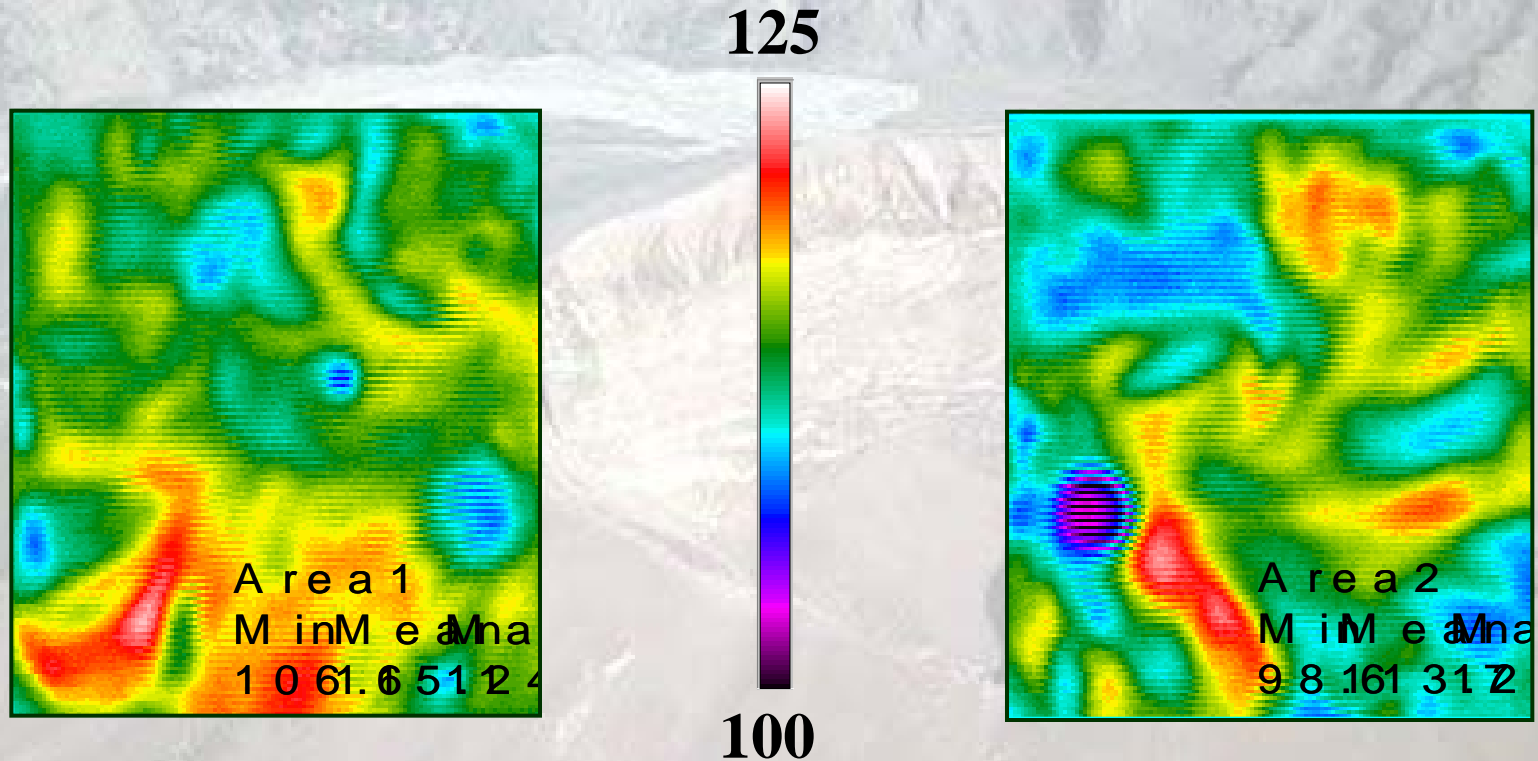
**QIRT
2012**

24

39

POOL BOLING

TEMPERATURE DISTRIBUTION ON THE HEATER



Water

Habon G

$q=100 \text{ kW/m}^2$

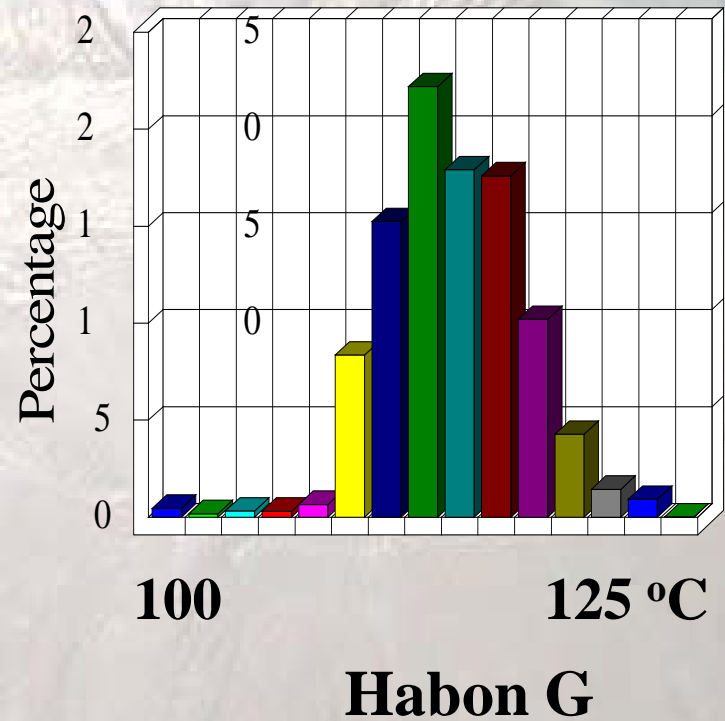
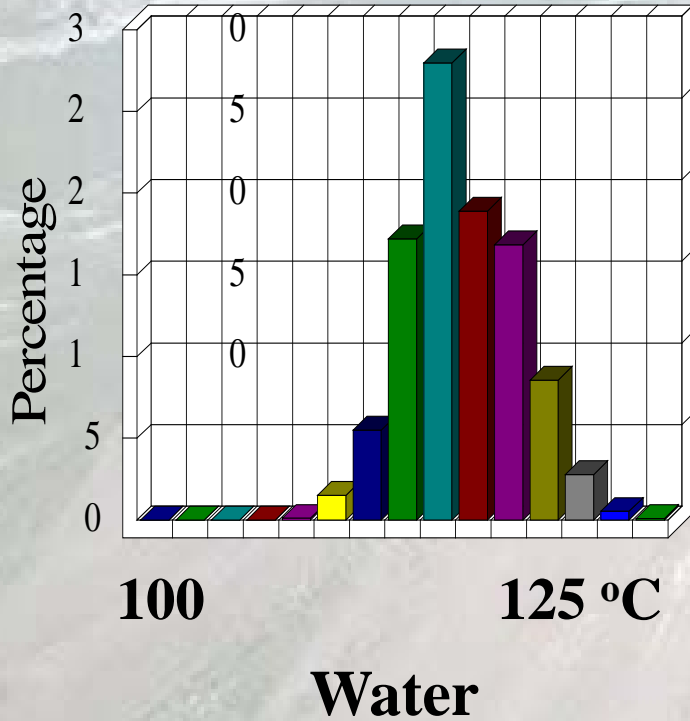
**QIRT
2012**

25
39

POOL BOILING

Temperature histograms

$$q=100 \text{ kW/m}^2$$

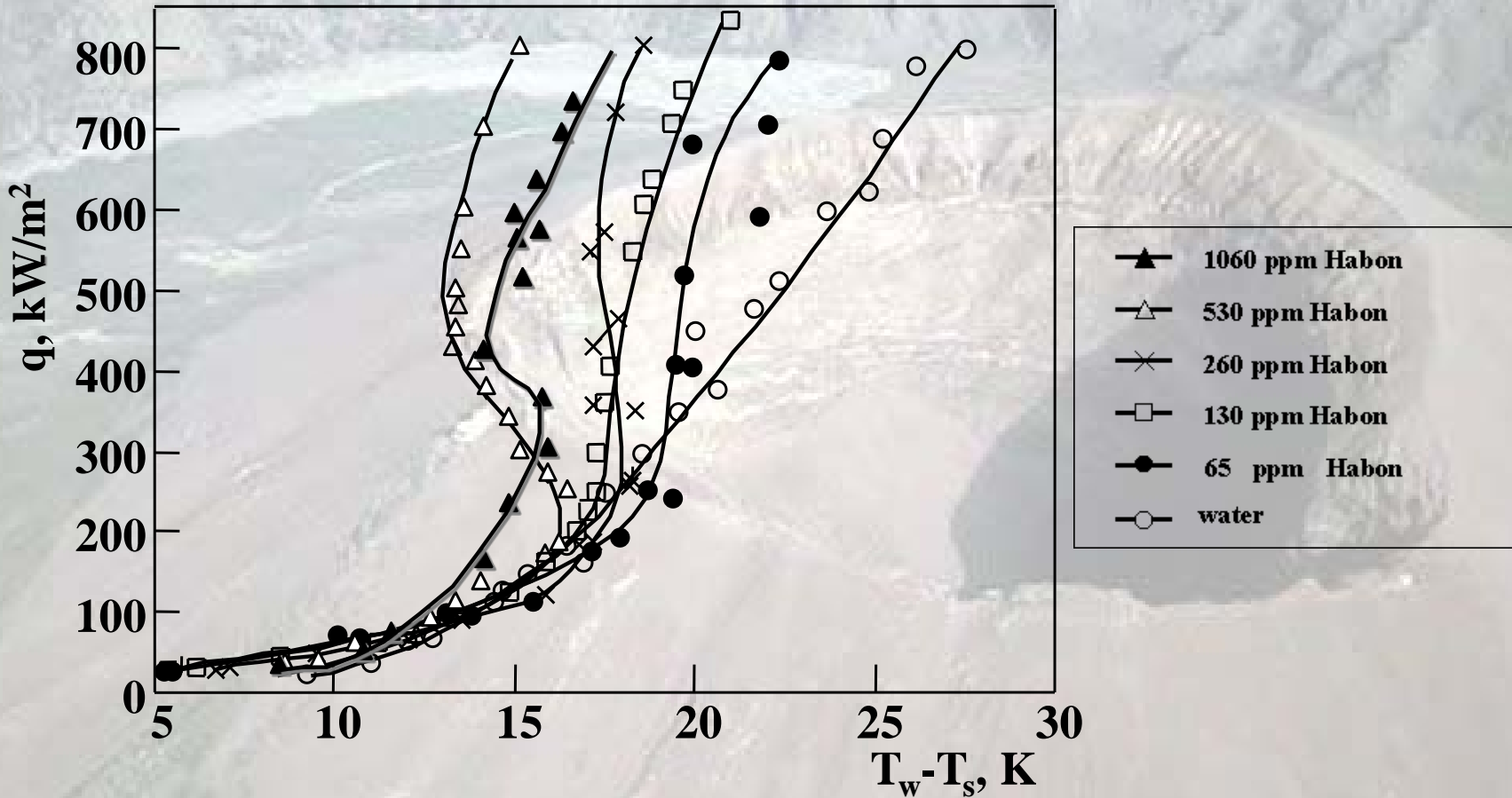


**QIRT
2012**

26
39

POOL BOILING

Habon G. Saturated boiling curves



**QIRT
2012**

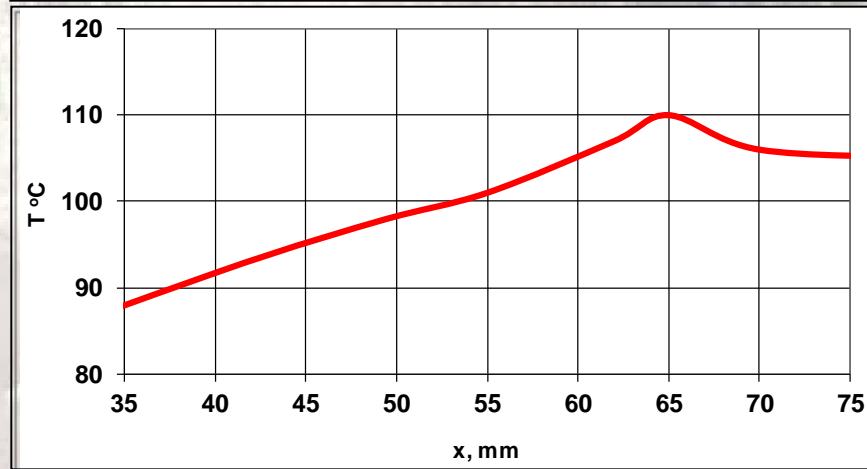
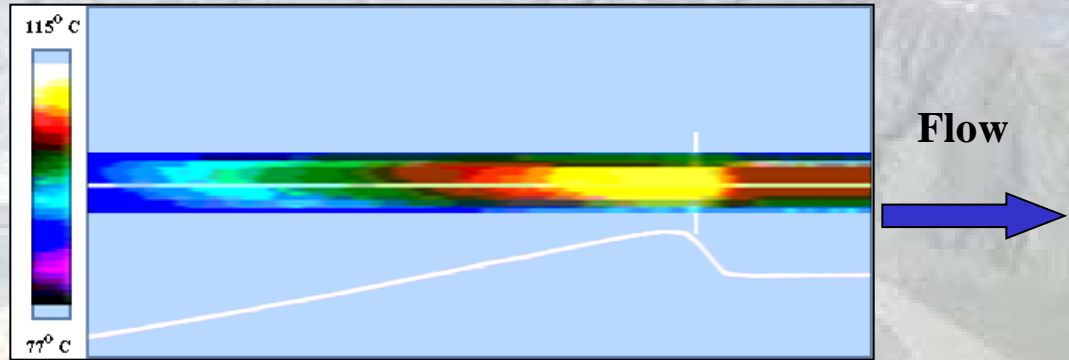
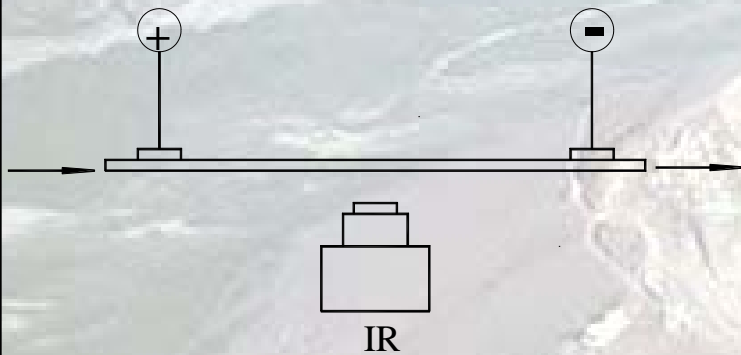
27

39

FLOW BOILING IN A CAPILLARY TUBE

$d_{in} = 1.07 \text{ mm}$

Experimental setup



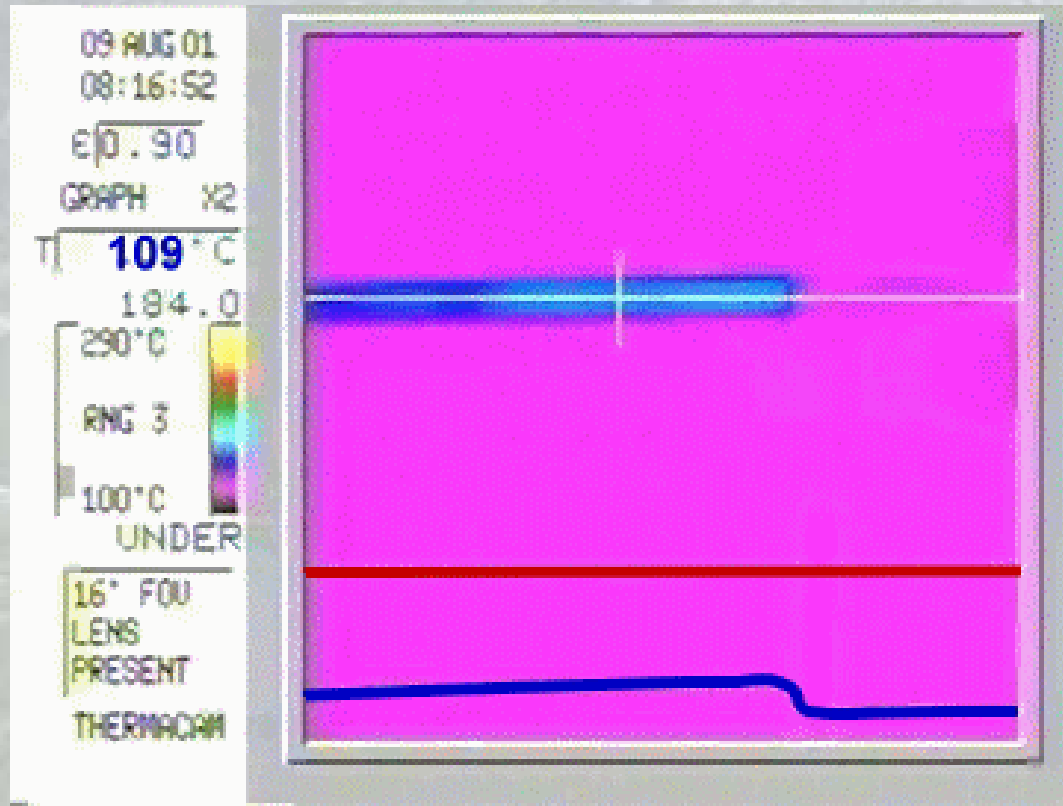
**Infrared image
and temperature distribution**

**QIRT
2012**

28
39

FLOW BOILING IN A CAPILLARY TUBE

$d_{in} = 1.07 \text{ mm}$



Flow
→

**Temperature
variation
on the
heated
wall**

Dryout

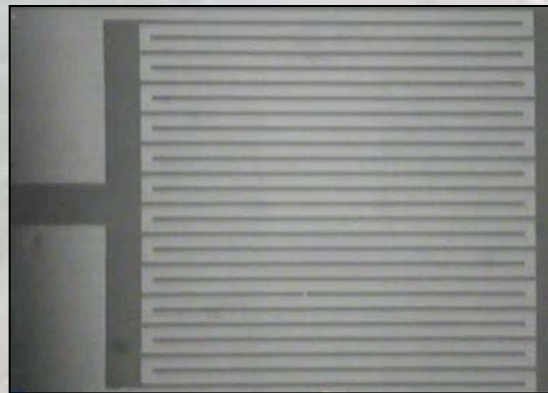
**QIRT
2012**

29
39

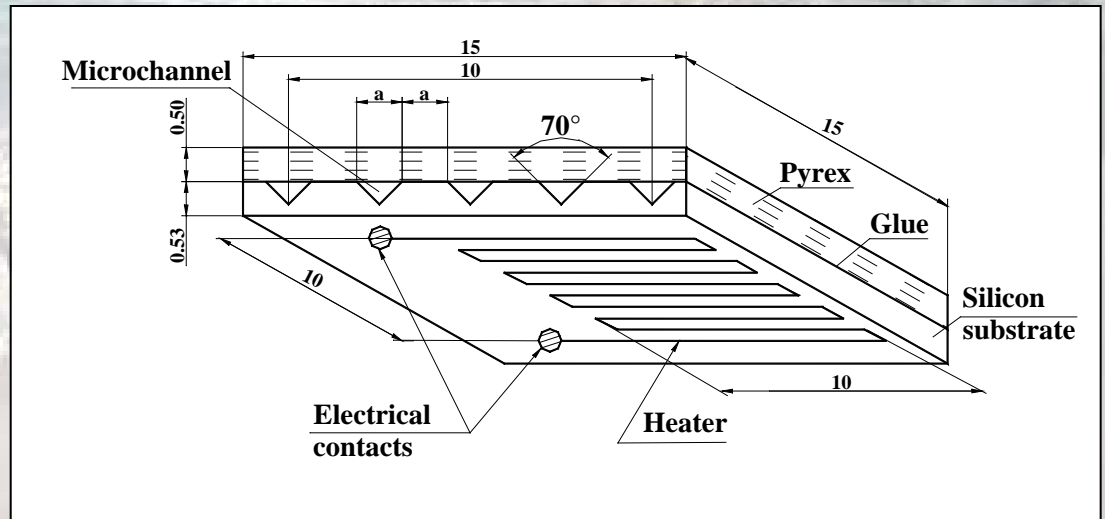
FLOW BOILING IN MICRO-CHANNELS THERMAL FIELD ON THE HEATER



micro-channels



heater

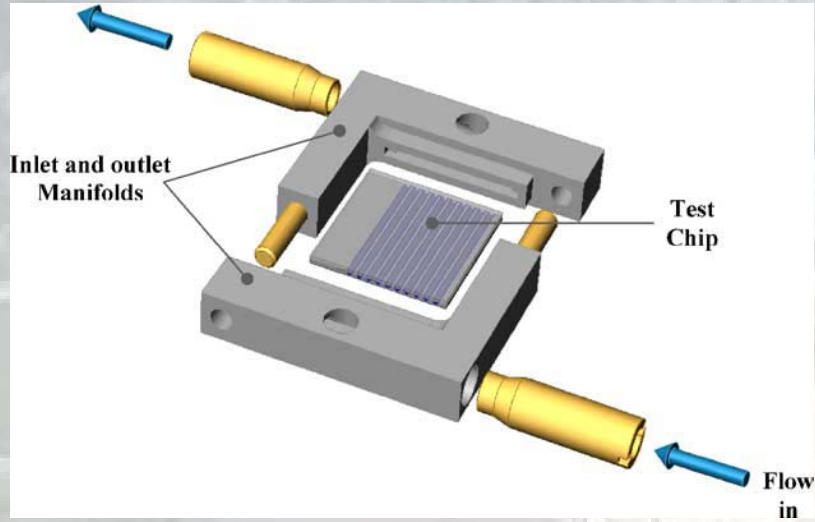


**QIRT
2012**

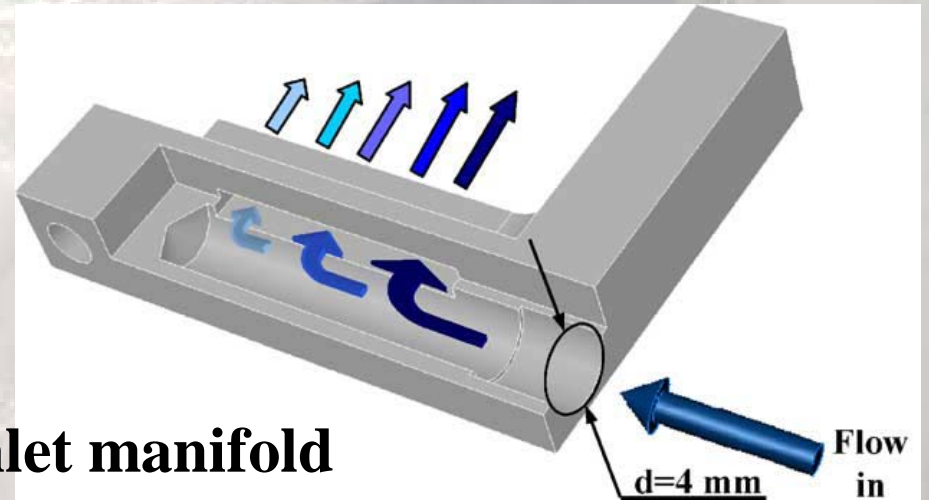
30

39

FLOW BOILING IN MICRO-CHANNELS THERMAL FIELD ON THE HEATER



Test module



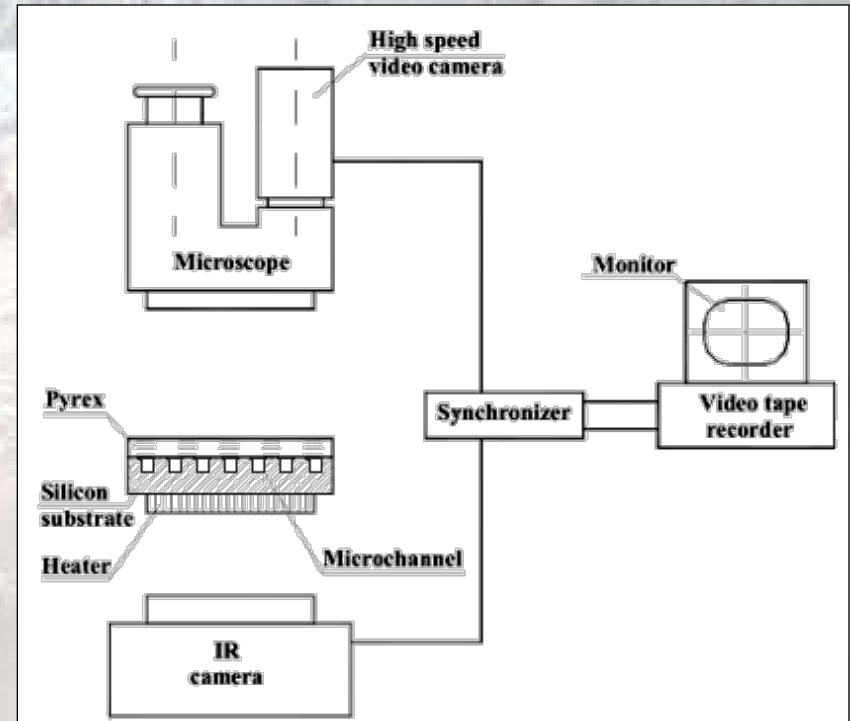
Schematic of the flow in the inlet manifold

**QIRT
2012**

31
39

FLOW BOILING IN MICRO-CHANNELS THERMAL FIELD ON THE HEATER

Experimental apparatus



**QIRT
2012**

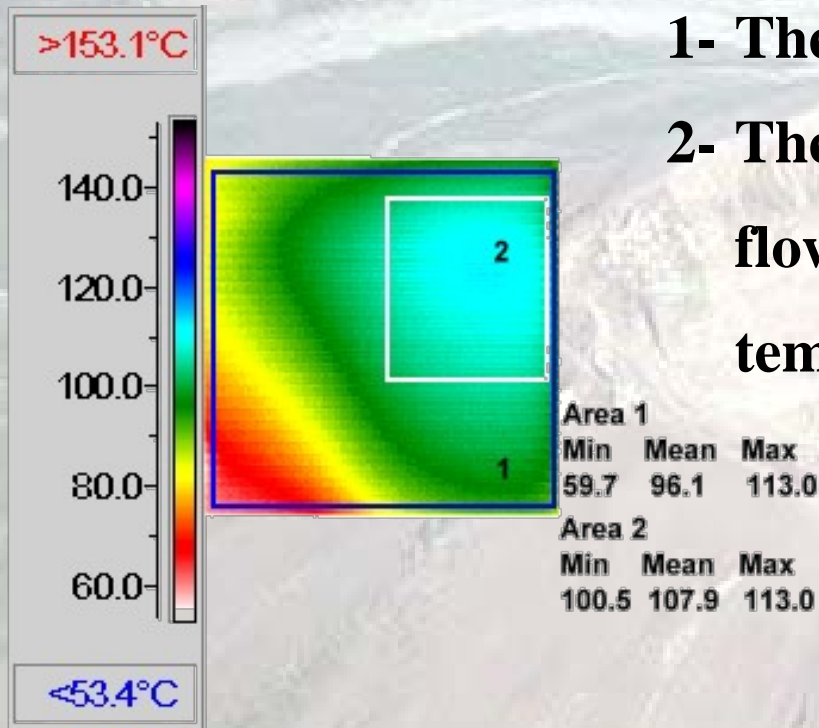
32
39

FLOW BOILING IN MICRO-CHANNELS THERMAL FIELD ON THE HEATER

$$\dot{m} = 95 \text{ kg/m}^2\text{s}, q=160 \text{ kW/m}^2, d_h=160 \text{ }\mu\text{m}$$

1- The area of the heater

2- The area of the heater, where saturated flow boiling occurs at mean wall temperature of $T_w=107.9 \text{ }^\circ\text{C}$



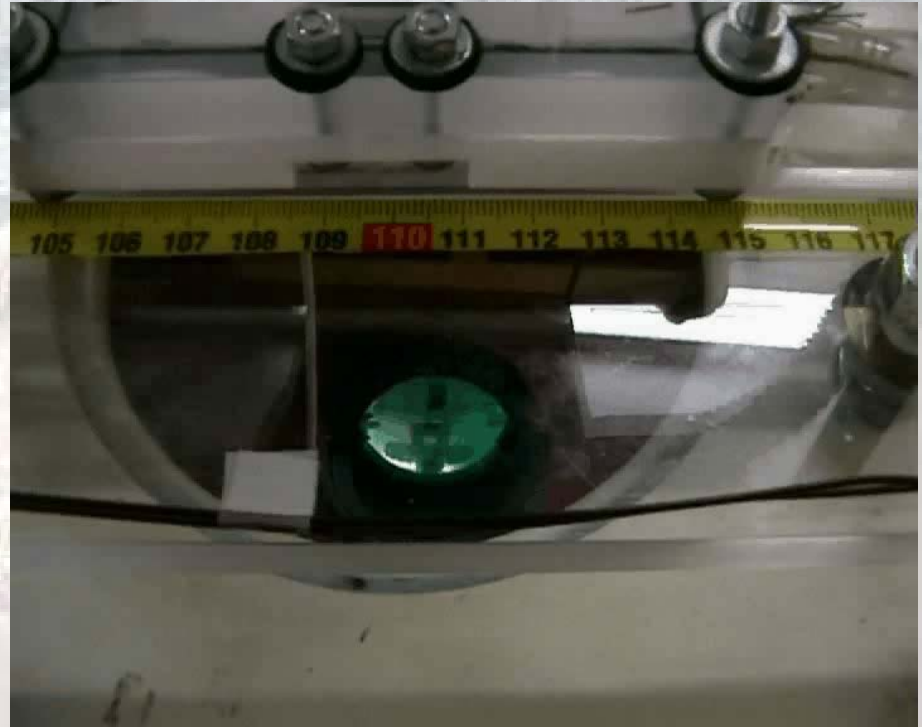
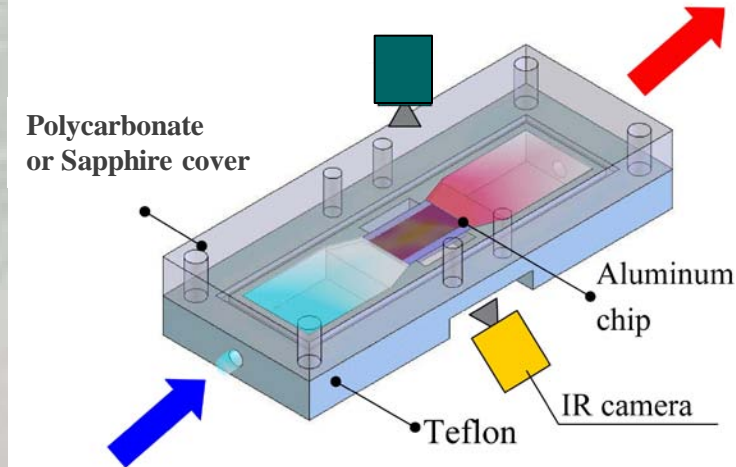
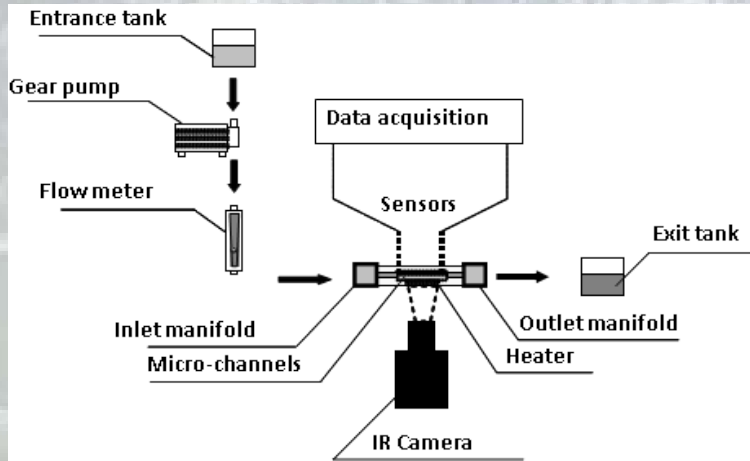
Measurements by non contact infrared thermography cover the whole temperature field

**QIRT
2012**

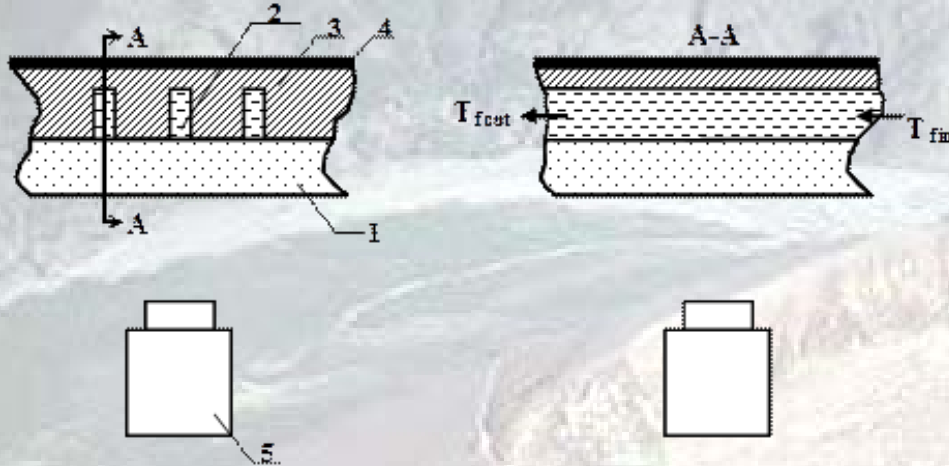
33
39

IR MEASUREMENTS IN THE LIQUID AND ON THE HEATER

Flow and thermal visualization



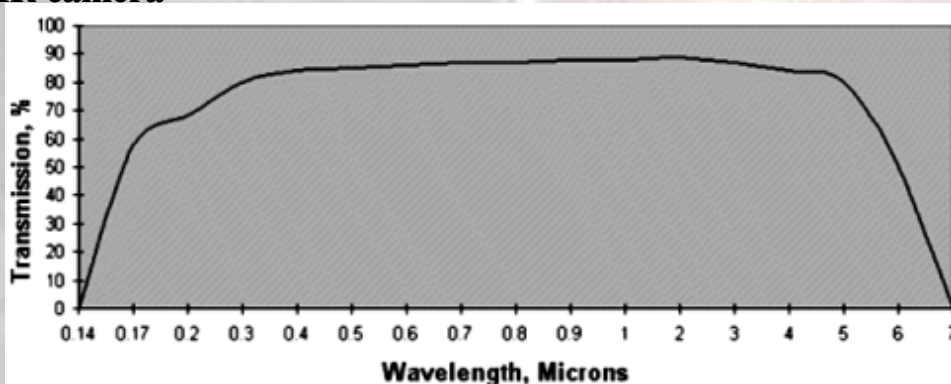
IR MEASUREMENTS IN THE LIQUID AND ON THE HEATER



The liquid is circulated in micro-channels (2) etched in the wafer (3). The heater (4) is attached to the top surface of the wafer (3). The micro-channel system is sealed by IR transparent window (1). The liquid temperature is measured by the IR camera (5) through this window.

Direct measurement of the liquid temperature through IR transmitted face layer.

- 1. IR transmitted face layer, 2. Micro-channel, 3. Wafer, 4. Heater, 5. IR camera



Transmission vs. wave length at 10 mm thickness of Sapphine glass

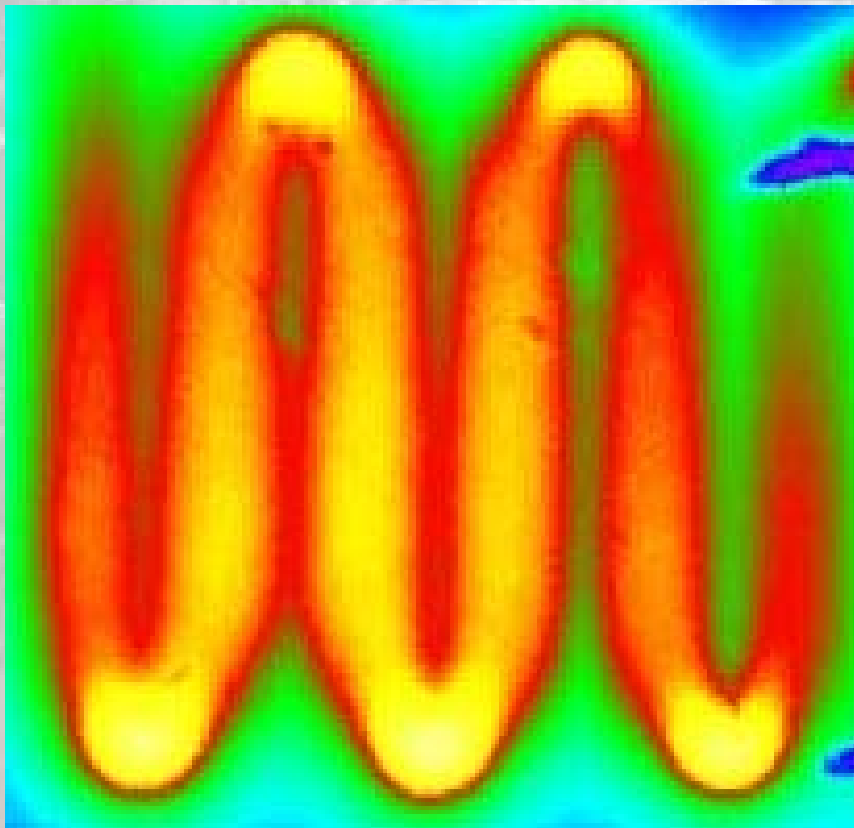
Y. Mishan, A. Mosyak, E. Pogrebnyak, G. Hetsroni, 2007, Effect of developing flow and thermal regime on momentum and heat transfer in micro-scale heat sink. *Int. J. Heat Mass Transfer* 50, 3100-3114.

**QIRT
2012**

35
39

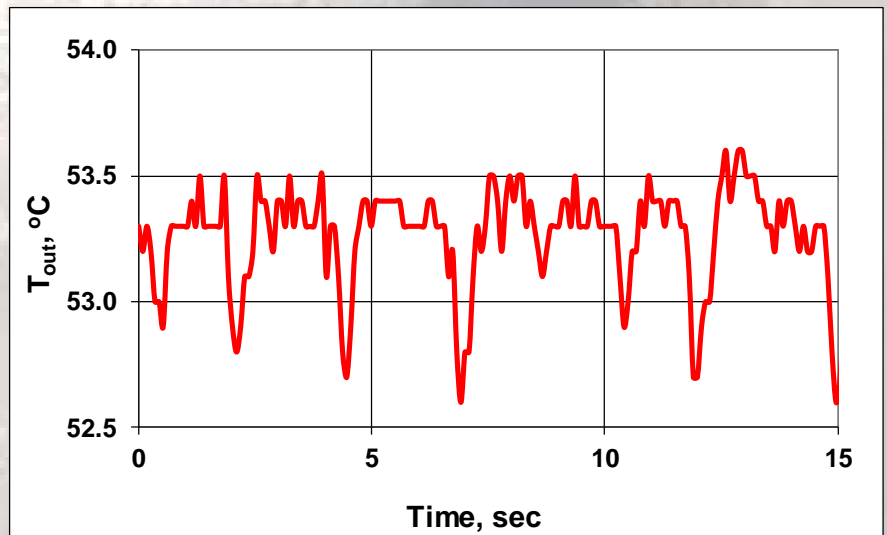
IR MEASUREMENTS IN THE LIQUID AND ON THE HEATER

Temperature oscillations on a heated wall



Serpentine heater 1×1 cm

Temperature

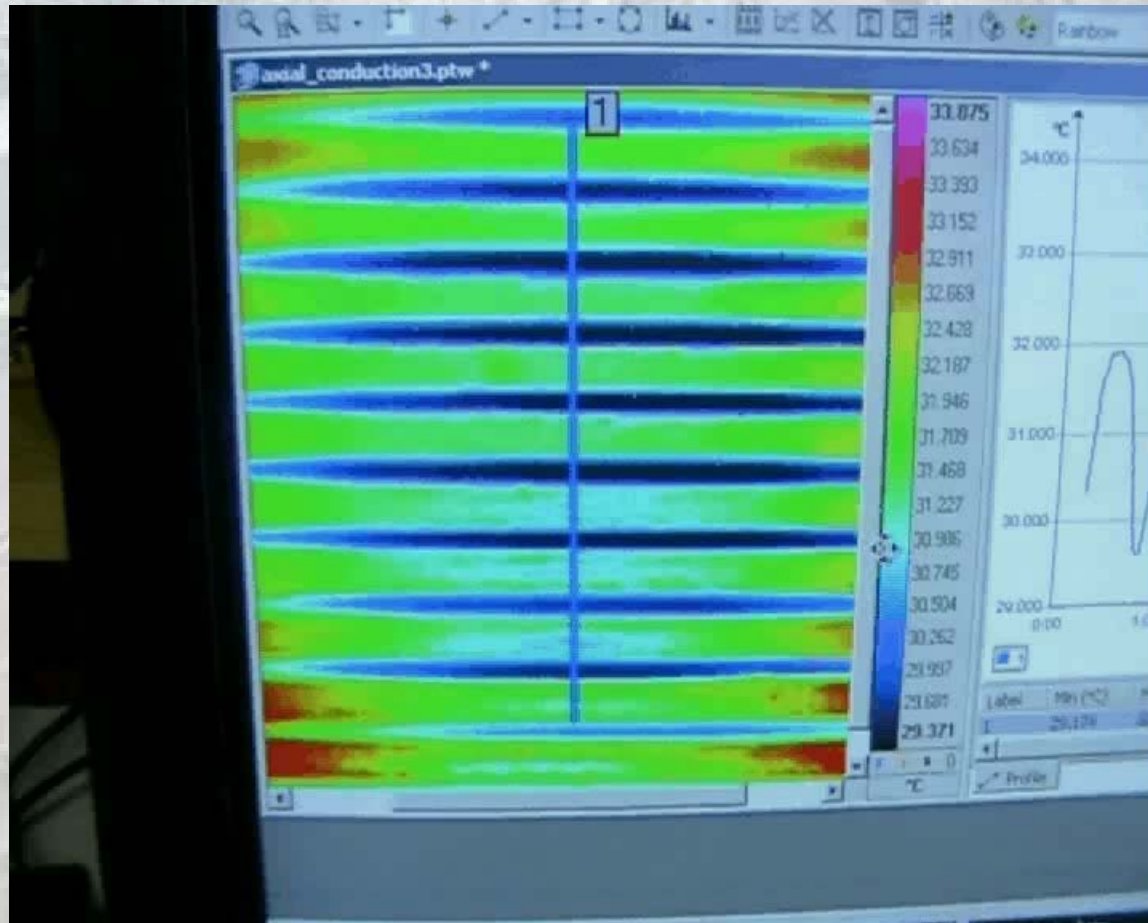


**QIRT
2012**

36
39

IR MEASUREMENTS IN THE LIQUID AND ON THE HEATER

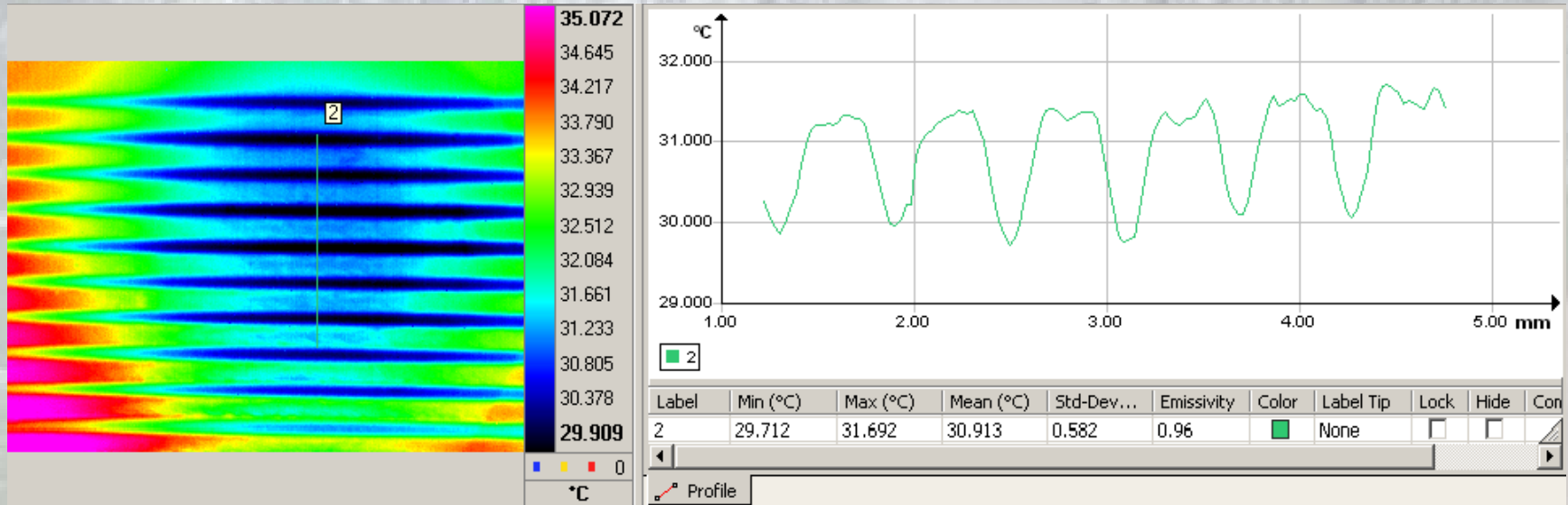
Measurements by IR camera inside the micro-channels



QIRT
2012

37
39

IR MEASUREMENTS IN THE LIQUID AND ON THE HEATER



Fluid temperature changes in the spanwise direction due to effect of channel walls temperature

**QIRT
2012**

38
39

CONCLUSIONS

Infrared thermography was used to detect the coherent structures, which originate in the buffer region of turbulent flow.

The thermal pattern on the heated wall for the single-phase flow has a streaky structure.

For air-liquid flow the streaky structure is destroyed. This phenomenon is accompanied by a significant increase in the heat transfer coefficient and sharp decrease in the temperature fluctuation values, whereas the level of pressure fluctuations almost did not change.

Flow boiling in parallel micro-channels is accompanied by quasi-periodical rewetting and refilling. Boiling of surfactant solutions in micro-channels may be used to provide a nearly isothermal heat sink

**QIRT
2012**

39

39

CONCLUSIONS

There is a reason to believe that using IR technique in ancient Rome could have saved the lives of many Pompeii citizens



The Last Day of Pompeii is a large painting by the Russian artist Karl Briullov (1830-33).

The painting is classical, with the use of chiaroscuro.

Karl Briulov was born on 12.12.1799 in St. Petersburg and buried 11.6.1852 near Rome.

He could not resist putting his image in the painting and even depicted his mistress in a somewhat compromising position.

| | | |
|----------------------|--|--|
| QIRT 2012 | | |
| | | |

**molti ringraziamenti
per l'attenzione**

